

Universität Ulm  
Institute für Angewandte Physiologie  
Prof. Dr. Dr. h. c. Frank Lehmann-Horn

Functional characterization of KCNJ2 mutations  
associated with Andersen-Tawil syndrome and atrial  
tachycardia

Dissertation  
zur Erlangung des Doktorgrades  
der Humanbiologie (Dr. biol. hum.)  
der Medizinischen Fakultät der Universität Ulm

vorgelegt von  
Georgeta Teodorescu  
Bukarest, Rumänien  
2007

Amtierender Dekan: Prof. Dr. Klaus-Michael Debatin

1. Berichterstatter: Prof. Dr. Stephan Grissmer

2. Berichterstatter: PD Dr. Karl Föhr

**Tag der Promotion: 24.07.2007**

## TABLE OF CONTENT

<b>1 INTRODUCTION</b> .....	1
<i>1.1 General description of potassium channels</i> .....	1
<i>1.2 Inward-rectifier potassium channels (Kir)</i> .....	2
1.2.1 Molecular assembly of Kir channels .....	2
1.2.2 Molecular structure of Kir channels .....	4
1.2.3 Physiological functions and expression of Kir channels .....	5
1.2.4 Mechanism and determinants of inward-rectification .....	5
<i>1.3 The Kir2 family of inward-rectifier potassium channels</i> .....	7
<i>1.4 Andersen-Tawil syndrome (ATS)</i> .....	9
1.4.1. Molecular genetics of ATS .....	10
<b>2 AIM OF THE STUDY</b> .....	11
<b>3 MATERIALS AND METHODS</b> .....	13
<i>3.1 Molecular biology methods</i> .....	13
3.1.1 Solutions and chemicals for molecular biology methods .....	13
3.1.2 DNA Clones .....	14
3.1.3 The transformation procedure .....	15
3.1.4 Plasmid DNA isolation and purification .....	16
<i>3.2 Cell culture</i> .....	17
3.2.1 Solutions and chemicals .....	17
3.2.2 Cell culture of COS-7 celline .....	17
3.2.3 Transfection .....	18
<i>3.3 Electrophysiology</i> .....	19
3.3.1 Solutions and chemicals for electrophysiology .....	19
3.3.2 Electrophysiological recordings and data analysis .....	19
<i>3.4 Confocal microscopy experiments</i> .....	20
<i>3.5 Structural modelling</i> .....	20
<b>4 RESULTS</b> .....	21
<i>4.2 Co-transfection experiments with WT and D78G mutant Kir2.1 channels</i> .....	23
<i>4.3 Properties of the R82W mutant Kir2.1 channels</i> .....	24
4.3.1 Co-transfection experiments of the R82W mutant Kir2.1 channels .....	24
4.3.2 Pharmacological characterization of the R82W mutant Kir2.1 channel .....	26
4.3.3 Effect of external Ba <sup>2+</sup> application on WT and R82W mutant Kir2.1 channels .....	28
<i>4.4 Co-transfection experiments with WT and V93I mutant Kir2.1 channels</i> .....	33

<i>4.5 Biophysical characterization of the G215 substitution in WT Kir2.1 channels</i> .....	35
4.5.2 Co-expression of WT with G215D mutant Kir2.1 channels .....	36
4.5.3 Co-expression of WT with G215R mutant Kir2.1 channels .....	38
4.5.4 Subcellular localization of WT and G215R mutant Kir2.1 channels .....	39
<b>5 DISCUSSION</b> .....	44
<i>5.1 The D78G mutation</i> .....	45
<i>5.2 The R82W mutation</i> .....	47
<i>5.3 The V93I mutation</i> .....	48
5.3.1 Mechanism of channel function increase by mutations in KCNJ2 .....	48
5.3.2 Consequences of channel function increase by mutations in KCNJ2 .....	49
<i>5.4 The G215R/D mutations</i> .....	49
5.4.1 Mechanism of channel function suppression by mutations associated with ATS.....	49
5.4.2 Consequences of channel function suppression by mutations in KCNJ2 .....	52
<i>5.5 Pathophysiology of clinical features in ATS</i> .....	52
5.5.1 Pathophysiology of the periodic paralysis.....	52
5.5.2 Pathophysiology of the cardiac arrhythmias .....	54
<b>6 SUMMARY</b> .....	56
<b>7 REFERENCE</b> .....	58

## ABBREVIATION

<b>A</b>	Adenine
Ba <sup>2+</sup> <sub>out</sub>	Extracellular barium
Å	Angstrom
AF	Atrial fibrillation
AP	Action potential
ATP	Adenosine-5'-triphosphate
ATS	Andersen-Tawil syndrome
Ba <sup>2+</sup>	Barium
<b>C</b>	Cytosine
Ca <sup>2+</sup>	Calcium
CaCl <sub>2</sub>	Calcium chloride
cDNA	Complementary Desoxiribonucleic acid
CMV	Multiple cloning vector site
COS-7	“Green African Monkey Kidney” cells
CPVT	Catecholaminergic Polymorphic Ventricular Tachycardia
D	Aspartic acid
DMEM	Dulbecco's modified Eagle's medium
<i>E. Coli</i>	Escherichia coli
ECG	Electrocardiogram - heart scan
EDTA	Ethylendiamin-tetra acetic acid;
EGTA	Ethylenglycol-tetra acetic acid;
$E_h$	The voltage at which half the channels are blocked
$E_K$	Equilibrium potential for potassium
EtBr	Ethidiumbromide
EtOH	Ethanol
FBS	Fetal Bovine Serum
<b>G</b>	Guanine
g	Gram
G	Glycine
GFP	Green fluorescent protein
GYG	Glycine-Tyrosine-Glycine
K <sup>+</sup> <sub>out</sub>	Extracellular potassium
HEPES	Piperazineethanesulfonic acid;
HypoPP	Hypokalemic periodic paralysis
<i>I</i>	Current
I	Isoleucine
I <sub>K1</sub>	Rectifier current
<i>k</i>	Steepness of block
K <sup>+</sup>	Potassium
Kb	Kilobase
KCl	Potassium chloride
KF	Potassium fluoride
Kir	Inward-rectifier potassium channel
KOH	Potassium hydroxide
Kv	Voltage gated potassium channels
l	Litter
LB	Luria Bertani
LQTS	Long QT syndrome
M	Mol/l

MEM	Minimum Essential Medium
MgCl <sub>2</sub>	Magnesium chloride
mM	Millimolar
mOsM	Osmolarity
ms	Milliseconds
mV	Millivolts
n	Number of cells
Na <sup>+</sup>	Sodium
NaCl	Sodium chloride
nm	Nanometer (10 <sup>-9</sup> meter)
No.	Number
NTP	Nucleotide
OD	Optical density
P	Pore
pA/pF	Picoampers/picoFarads
PBS	Phosphate buffered saline
PCR	Polymerase chain reaction;
pH	“Potential of hydrogen”
PIP2	Phosphatidylinositol-4,5-bisphosphate;
R	Arginine
RMP	Resting membrane potential
RNA	Ribonucleic acid
rpm	Rotation per minute
S.E.M	Standard error of the mean
SDS	Sodium dodecyl sulphate
SUR	Sulfonylurea receptor
<b>T</b>	Thymine
T	Tyrosine
TBA	Tris Borate EDTA
TE	Tris EDTA
Tris	Tris(hydroxyethyl)aminomethan
V	Valine
VF	Ventricular fibrillation
Vol	Volume
VT	Ventricular tachycardia
W	Tryptophan
WT	Wild type

# 1 INTRODUCTION

## 1.1 General description of potassium channels

Ion channels play a fundamental role in cell physiology. They are transmembrane proteins involved in cell excitability, in modulation of muscle cell contractility, and in the release of hormones and neurotransmitters from endocrine and neuronal cells. Gating of these proteins occurs through conformational changes that are controlled by voltage and/or ligand binding (Jiang *et al.*, 2003 a).  $K^+$  channels represent the largest and most diverse group of channels.

Based on the structural organization of their subunits,  $K^+$  channels can be divided in several classes (Fig. 1). The class consisting of subunits with one pore domain per subunit and six transmembrane segments (6TMS) includes families of voltage-gated ( $K_v$ ) and  $Ca^{2+}$ -activated  $K^+$  channels (Fig. 1, column 1). The class consisting of proteins with two transmembrane segments (2TMS) and one pore domain per subunit includes the family of inward-rectifier  $K^+$  channels (Kir) (Fig. 1, column 2). Another class, known as the class of two-pore domain  $K^+$  channels comprises  $K^+$  channel subunits with four (4TMS) (Fig. 1, column 3) or eight transmembrane segments (8TMS) (Fig. 1, column 4). The 4TMS class includes families of “leak”  $K^+$  channels. Each of these families of  $K^+$  channels can further be divided into sub-families that comprise several  $K^+$  channel members.

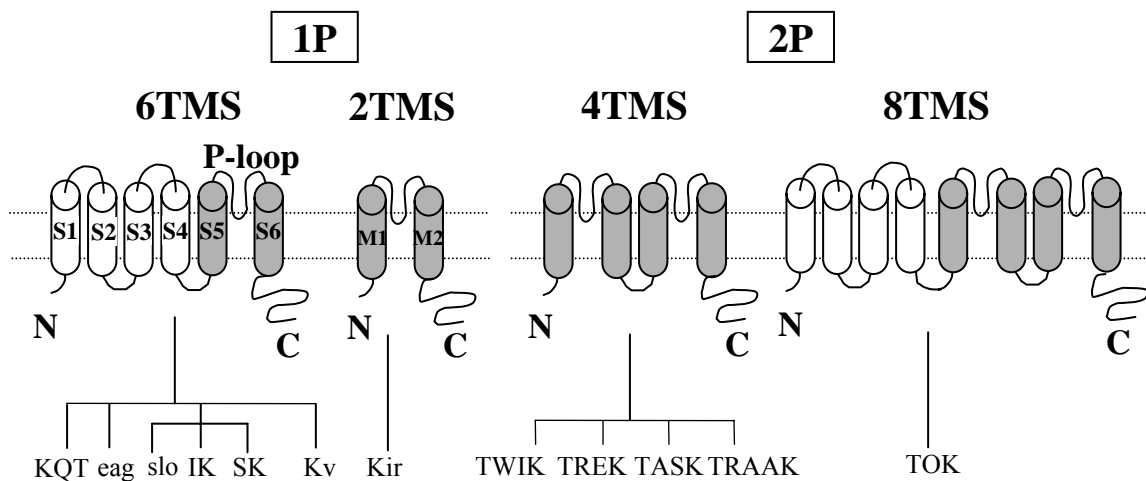


**Fig. 1. Schematic classification of  $K^+$  channel subunits.**  $K^+$  channels are divided in classes based on their transmembrane topology of their subunits. Channels exist with 6TMS/1P (six transmembrane segments/one pore), 2TMS/1P, 4TMS/2P and 8TMS/2P. N- and C-terminal are located intracellularly.

In 6TMS K<sup>+</sup> channels four subunits (S1-S6) have to assemble to form a functional tetrameric channel. The pore of the channel is formed by S5 and S6 and the P-loop between them (Doyle *et al.*, 1998; Jiang *et al.*, 2003 a). The P-loop that connects S5 and S6 contains the selectivity filter, known as the GYG motif. As this K<sup>+</sup> channel signature sequence is conserved between all K<sup>+</sup> channels it is assumed that the mechanism of ion selectivity and permeation at the selectivity filter is similar in all K<sup>+</sup> channels.

Although the other segments (S1-S4) of the channel are not directly involved in ion selectivity, they also play important roles. For example, the S4 is known as the voltage sensor in Kv channels, responsible for opening of channels upon depolarization (Jiang *et al.*, 2003 a, b), the N-terminal segment contains a tetramerization domain (T1) necessary for the correct assembly of the Kv tetramers (Babila *et al.*, 1994) and the C-terminal segment contains the calmodulin-binding domain important for the activation of pure Ca<sup>2+</sup>-dependent K<sup>+</sup> channels (Fanger *et al.*, 1999).

In contrast to the tetrameric association formed by the assembly of four 6TMS/1P channel subunits in the plasma membrane, the 4TMS/2P (Glowatzki *et al.*, 1995) and, the 8TMS/2P channel subunits only need to dimerize to form a functional channel

In analogy with 6TMS/1P, the 2TMS/1P class of K<sup>+</sup> channels requires a tetrameric arrangement (MacKinnon, 1991; Yu and Catterall, 2004) of four P-regions to form a K<sup>+</sup> selective pore. Inward-rectifier K<sup>+</sup> channels (Kir) are structured as follows: each subunit has two transmembrane segments (M1 and M2) flanking a pore-forming loop (H5) homologous to the P-loop of Kv channels. M1 and M2 segments are homologous to S5 and S6, respectively from Kv channels. Kir channels can be formed by co-assembly of homo- or heteromeric Kir subunits (Yang *et al.*, 1995), which endows channels with distinct properties and further increases their functional diversity (Butt and Kalsi, 2006).

## ***1.2 Inward-rectifier potassium channels (Kir)***

### **1.2.1 Molecular assembly of Kir channels**

The 2TMS/1P class of K<sup>+</sup> channels (Kir) shortly described in the previous chapter, have been classified on the basis of sequence homology into seven sub-families, Kir1 to Kir7 (Fig. 2) (Doupnik *et al.*, 1995; Lopatin and Nichols, 1996).

The channel proteins share about 40 % homology among the Kir sub-families and >60 % within the sub-families. Kir channel subunit assembly was shown by a functional approach of homo- or heterotetrameric Kir channels (Glowatzki *et al.*, 1995) or by biochemical experiments (Yang *et al.*, 1995). Some Kir subunits require co-assembly with other Kir subunits in order to form functional channels (Fakler *et al.*, 1996).

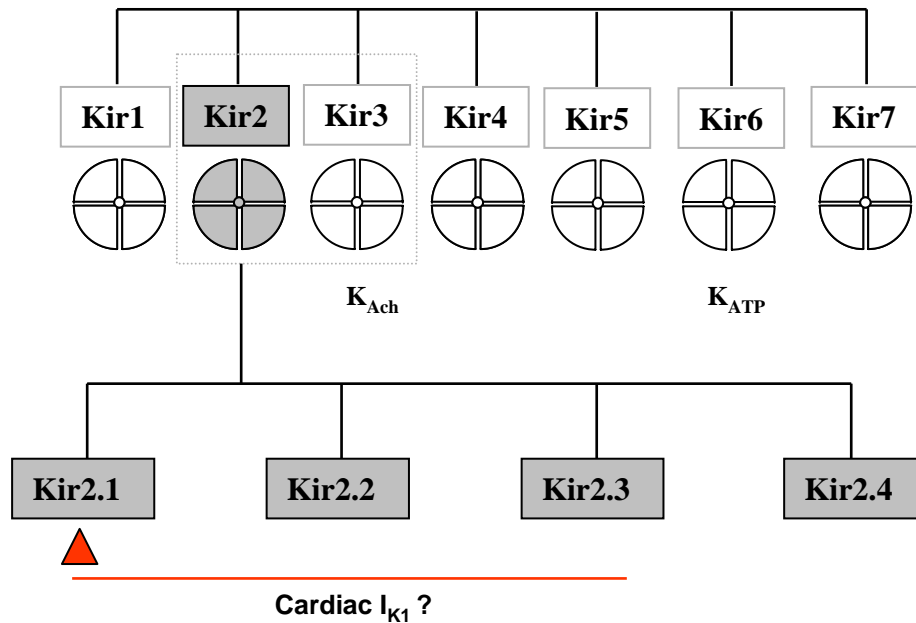


**Fig. 2. Molecular structure of Kir channels.** Seven Kir sub-families (Kir1-7) have been described. All Kir channels are tetrameric proteins of 2TMS/1P domain subunits that equally contribute to the formation of highly selective  $K^+$  channels. Most Kir channels can be assembled in functional homotetramers while some require heteromeric assembly (Fakler *et al.*, 1996).

Formation of heteromeric channels seems to underlie several Kir conductances of physiological importance. For instance, Kir3.1/Kir3.4 heterotetrameric channels closely resemble the native atrial current  $I_{K1,ACh}$  (Krapivinsky *et al.*, 1995). The tetrameric nature of Kir channels (Yang *et al.*, 1995) leads to the theoretical possibility of one gene product co-assembling with another gene product to form heteromultimeric channels. Heteromultimeric complexes have been found in the mammalian heart and brain (Krapivinsky *et al.*, 1995). The principles determining whether channel subunits assemble predominantly with themselves or with other members of the gene family are thus of great importance. However, the rules governing assembly in Kir channel subunits have not yet been established (Tinker *et al.*, 1996). Maybe the molecular structure of Kir channels could shed light onto the mechanism responsible for Kir channel subunit assembly.

### 1.2.2 Molecular structure of Kir channels

The crystal structure of KirBac1.1 and KcsA gave insights into the architecture of Kir channels, because they both have two transmembrane spanning helices per subunit.

Recently, the high-resolution structure of KirBac1.1, a bacterial ion channel that is closely related to eukaryotic Kir channels was solved in its closed conformation (Kuo *et al.*, 2003) (Fig. 3). In accordance with nomenclature describing the KirBac1.1 channel structure the N-terminal part of the P-loop is  $\alpha$ -helical and forms the shallow outer vestibule of the channel. Ion selectivity is determined by a narrow binding site in the pore termed selectivity filter which is formed by the backbone carbonyls of the GYG motif.

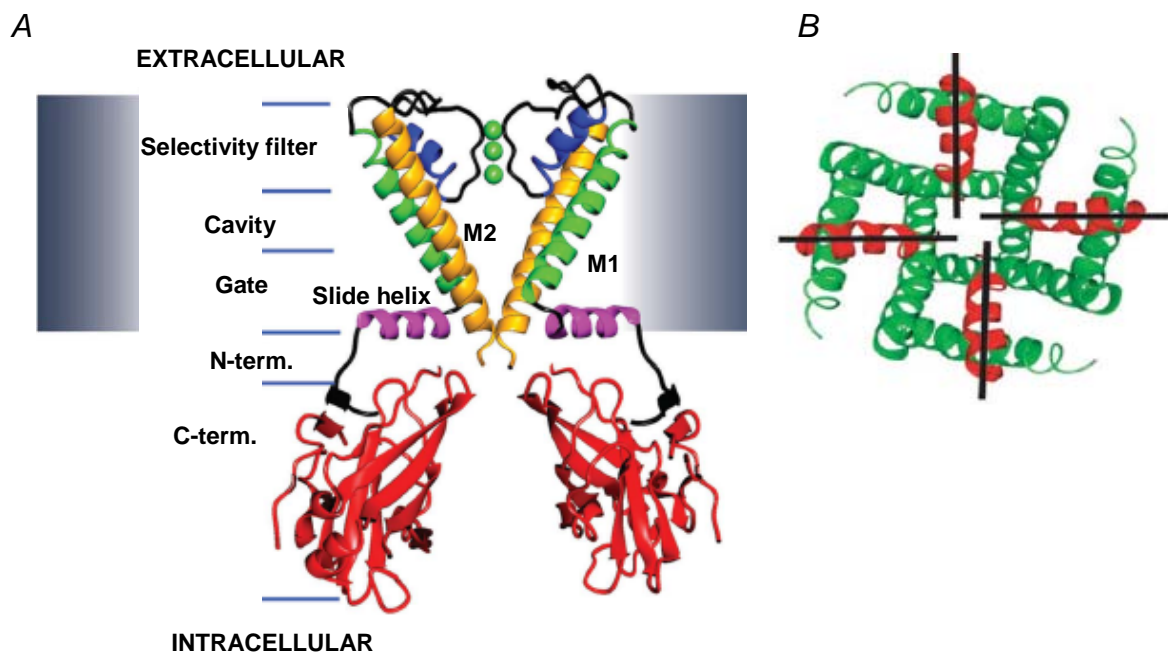


**Fig. 3. Overview of the KirBac1.1 structure.** The position of the membrane is represented by the shaded bar. *A* Two subunits are shown for clarity so that positions of the following structural elements can be seen: slide helix (pink), outer helix M1 (green), pore helix (blue), inner helix M2 (yellow), and C-terminal domain (red). *B* Relative positions of the pore helices are depicted in red in the crystal structure of KirBac1.1. This is viewed from the extracellular side of the channel looking directly down the central ion conduction pathway. Black lines through the centre of each pore helix indicate their orientation relative to the centre of the cavity.

The outer helix M1 (Fig. 3, A, green) lines the pore and is tilted around M2 (Fig. 3, A, yellow). The long and narrow inner vestibule is formed by residues of the M2 helix and contains binding sites for  $K^+$  and small blocking ions. Compared with the structure of KcsA channel, an extra helix, named the slide helix (Fig. 3, A, violet) is present in the

transmembrane section of the KirBac1.1 structure. This slide helix runs parallel to the cytoplasmic face of the membrane. As determined by X-ray crystallography the KirBac1.1 structure consists of  $\alpha$ -helical integral membrane structures plus intracellular region consisting mostly of  $\beta$  sheet which forms the cytoplasmic pore (G-loop). This region is crucial for channel modulation by intracellular regulators and for establishing the strong voltage dependence of inward rectification.

The high sequence homology between KirBac1.1 and eukaryotic Kir channels (Kuo *et al.*, 2003; Durell *et al.*, 1994) makes it easier to evaluate interactions deduced from functional assays in the context of the relevant channel structure and function.

### **1.2.3 Physiological functions and expression of Kir channels**

Kir channels are expressed in a wide variety of cell types including neuronal cells, myocytes, blood cells, skeletal muscle fibres, macrophages, osteoclasts, endothelial and placental cells (Doupnik *et al.*, 1995; Raab-Graham and Vandenberg, 1998).

They maintain the membrane potential near the equilibrium potential for  $K^+$  ( $E_K$ ) in excitable and non-excitable cells (Hille, 1992; Doupnik *et al.*, 1995). Modulation of these channels can therefore alter the membrane potential, cellular excitability, heart rate, information processing and secretion of neurotransmitters or hormones (Chung *et al.*, 1997; Isomoto and Kurach, 1997; Reimann and Ashcroft, 1999). In the central nervous system, Kir channels contribute to the resting potential and to synaptic potentials (Nicoll *et al.*, 1990; Premkumar and Gage, 1994). Kir channels are also important in proliferation, differentiation and, survival of neurons and glial cells.

The Kir current was first observed electrophysiologically in frog skeletal muscle by Katz in 1949 (Katz, 1949) and named an anomalous rectifier due to its unique properties (the larger conduction of  $K^+$  ions in the inward direction compared to the outward direction) which were in contrast to the known voltage-dependent delayed-rectifier  $K^+$  channels. The unique properties of Kir channels will be described in more detail in the following chapter.

### **1.2.4 Mechanism and determinants of inward-rectification**

The electrophysiological properties of Kir channels include, as their name implies, the conduction of larger inward currents compared to outward current (Hille, 1992). This is due to a reduced open probability when the membrane potential is more positive than the

$K^+$  equilibrium potential (Hille, 2001). Consequently, despite their name, under physiological conditions Kir channels primarily conduct outward  $K^+$  currents. Inward rectification is primarily caused by a voltage-dependent block of outward currents by intracellular blockers such as  $Mg^{2+}$  and polyamines (Vanderburgh *et al.*, 1987; Ficker *et al.*, 1994; Lopatin *et al.*, 1994; Fakler *et al.*, 1996). The extent of rectification varies among different sub-families which may be ‘weak’ or ‘strong’ (Hille, 1992). The stronger rectification of Kir2 can be partly explained by negatively charged residue in the M2 segment, D172 (Lu and MacKinnon, 1994; Stanfield *et al.*, 1994; Wible *et al.*, 1994; Fakler *et al.*, 1996) and Glu224 and Glu299 in the cytoplasmic C-terminal domain of the channel (Yang *et al.*, 1995; Kubo and Murata, 2001). However, the high degree of rectification among different Kir channels does not directly relate to the presence of these negative charges. For example, Kir7.1 shows weak rectification but has a negative charge in the M2 domain. Kir3.2 shows strong rectification but lacks the same negative charge (Finley *et al.*, 2004). Inward-rectification is prominent at high pH, while at low pH rectification is very weak in Kir1.1 channel. In some Kir channels the G-loop plays a role in the rectification process. The G-loop (residues: 300-315) is a conformational structure that is believed to form a flexible barrier for  $K^+$  permeation at the apex of the cytoplasmic pore (Pegan *et al.*, 2005).

### **1.2.5. Cytoplasmic regulatory factors**

In addition to rectification, regulation by membrane phospholipids is another common feature of Kir channels. Opening of Kir channels requires phosphatidylinositol 4,5-bisphosphate ( $PIP_2$ ) binding to basic and polar amino acids in the cytoplasmic segment, whereas depletion of  $PIP_2$  seems to close the channel (Shyng *et al.*, 2000; Lopes *et al.*, 2002).  $PIP_2$  is required to stabilize the open state of Kir channels (Huang *et al.*, 1998). It binds directly to Kir channels through the interaction between positively charged amino acids of the Kir channel and negatively charged phosphate groups of the lipid. Soom *et al.* (2001) described in the C-terminal region of Kir2.1 channels three independent  $PIP_2$  binding sites.

Conformational changes in the G-loop (V302 Kir2.1) may indirectly influence  $PIP_2$  gating (Ma *et al.*, 2007). The highly conserved residues in the cytoplasmic C-terminus (Nishia & MacKinnon, 2002) suggests a common structural feature for gating Kir channels, yet the cytoplasmic segments respond differently to intracellular regulatory signals. For example,

Kir2.1 channels remain open through endogenous PIP<sub>2</sub> binding, whereas Kir3 channels are opened by G proteins and Kir6 channels are closed by intracellular ATP, respectively.

Homology modelling of KcsA and KirBac1.1 channels suggested the interaction between specific blockers and the pore could be located at the cytosolic portion of the inner helix named ‘bundle crossing’ region. Two locations for the intrinsic gate of Kir channels have been proposed: the ‘bundle crossing’ (Perozo *et al.*, 1999) and the ‘selectivity filter’. A study of the localization of the PIP<sub>2</sub> activation gate in Kir channels based on the similar topology to KcsA channels (Xiao *et al.*, 2003) suggested that the M2 helices of Kir2.1 do undergo conformational changes upon PIP<sub>2</sub> binding and unbinding.

In Kir channels, structural features other than the GYG sequence were also important for K<sup>+</sup> selectivity. In most Kir channels, a salt bridge between conserved charged residues in adjacent subunits had been suggested to anchor and stabilize the K<sup>+</sup> channel signature sequence (Yang *et al.*, 1997; Kubo, 1996; Shieh *et al.*, 1999; Dibb *et al.*, 2003). Even changes within the K<sup>+</sup> channel signature sequence could affect gating rather than selectivity (Asmole *et al.*, 2001; Lu *et al.*, 2001). There is accumulating evidence that the selectivity filter and the outer pore of Kir channels undergo conformational changes during gating (Chapener *et al.*, 2000, 2002 and 2003; Lu *et al.*, 2001; Choe *et al.*, 1998; Guo & Kubo, 1998; Proks *et al.*, 2003; Chan *et al.*, 1996; Lu *et al.*, 2001).

Recently, in studies of two Kir channels, rat Kir3.1 and bacterial KirBac1.1 (Kuo *et al.*, 2003) a structure was postulated that phenylalanine at position 146 located within the pore-facing M2 helices forms a barrier to ion permeation, similar to the ‘helix bundle crossing’ in KcsA or in Kir3.4, to control the pore aperture. However, gating of eukaryotic Kir channels (Kir2.1, Kir3 and Kir6) requires additional elements (Proks *et al.*, 2003) such as ATP and G<sub>βγ</sub>, (G protein subunits).

### ***1.3 The Kir2 family of inward-rectifier potassium channels***

Members of the K<sup>+</sup> channel gene sub-family Kir2 encode pore-forming subunits of the strong inward rectifier K<sup>+</sup> channels (Kir2).

Kir2 channels are important in the modulation of cell excitability, repolarization of the action potential (AP), and determination of the cellular resting potential. Therefore, Kir2 channels are considered key components in the control of neuronal excitability in brain, electrical activity in the heart, vascular tone, and glial buffering of K<sup>+</sup> (Lopatin and Nichols, 1996; Isomoto *et al.*, 1997).

To date, four Kir2 subunits have been identified (Kir2.1-Kir2.4) in a variety of tissues. Three of these subunits (Kir2.1-Kir2.3) are expressed in cardiac cells (Melnyk *et al.*, 2002; Miake *et al.*, 2003; Zobel *et al.*, 2003), vascular smooth muscle cells (Zaritsky *et al.*, 2000; Karkanis *et al.*, 2003), and neurons (Neusch *et al.*, 2003), whereas expression of Kir2.4 has been reported only in neuronal cells (Perier *et al.*, 1994).

Kir.2 channels mediate the inward rectifier current ( $I_{K1}$ ) in the heart (Lopes *et al.*, 2002).  $I_{K1}$  is considered to contribute significantly to repolarization currents during the terminal phase of the AP and serves as the primary conductance controlling the resting membrane potential (RMP) in ventricular myocytes. Near the RMP, the  $I_{K1}$  conductance is the largest current in ventricular myocytes compared to any other conductance in the cells. It is thus likely that modulation of the  $I_{K1}$  current will have a significant effect on excitability. In addition to differences in current density, atrial and ventricular  $I_{K1}$  have differences in outward current profiles and in extracellular potassium  $[K^+]_{out}$  dependence. The whole-cell patch clamp technique was used to study the Kir2.x channel properties in heterologous expression systems. Kir2.1 and Kir2.2 heterotetrameric channels showed no outward current at potentials more positive than -30 mV. In contrast, outward current was still observed in homomeric Kir2.3 channels at more positive potentials than -30 mV (Dhamoon *et al.*, 2004).

Kir2 channels are important for cardiac function; the small efflux of  $K^+$  ions helps drive the cell's resting potential towards  $E_K$ , thereby reducing membrane excitability (Lopatin *et al.*, 1994). Additionally, in the brain, mouse knockout studies have shown that the lack of Kir2.1 channels produced vasoconstriction in cerebral blood vessels (Lopatin and Nichols, 1996).

The Kir2.1 channel plays a major role in setting the RMP and modulating the AP waveform (Davies *et al.*, 2005). Aberrant activity of Kir channels has been related to disorders and will be described in the following chapter.

### **Mutations in Kir channels associated with disease conditions**

Dysfunctions of Kir channels have been related to a variety of endocrine diseases (persistent hyperinsulinaemic hypoglycaemia of infancy) (Thomas *et al.*, 1995 and 1996), neurological disorders: for e.g., loss of Kir3 channels leads to hyperexcitability and seizures in the brain (Signorini *et al.*, 1997), cardiac abnormalities (Wickman *et al.*, 1998), hyperactivity and reduced anxiety (Blendnov *et al.*, 2001).

Mutations in Kir1 channels have been implicated for Bartter syndrome (Derst *et al.*, 1997) and mutations in Kir2.1 channels have been associated with Andersen-Tawil syndrome (Andersen *et al.*, 1971) and will be described in more detail in the following chapters.

#### ***1.4 Andersen-Tawil syndrome (ATS)***

ATS, first described in 1971 (Andersen *et al.*, 1971), is a human ion channel disorder (channelopathy), characterized by periodic paralysis, cardiac arrhythmias and skeletal anomalies (Tawil *et al.*, 1994).

It has recently been determined that at least one form of ATS is caused by a mutation in a potassium ion channel. Since its original description of genetic defects in 2001, more than 30 mutations have been identified in the KCNJ2 gene. However, it could be that other mutations in other proteins, which are yet to be identified, are responsible for ATS.

Between 6-20 % of individuals with identified KCNJ2 mutations appear phenotypically normal (non-penetrant).

Additionally, approximately 20 % of patients with ATS do not harbour KCNJ2 mutations (Tawil *et al.*, 1994; Alagem *et al.*, 2001; Plaster *et al.*, 2001; Tristani-Firouzi *et al.*, 2002; Donaldson *et al.*, 2003; Yoon *et al.*, 2006, Sansone and Tawil 2007). This suggests that the disease must be genetically heterogeneous or other factors, such as regulatory proteins, may alter Kir2.1 function.

Patients with mutations associated with ATS exhibit periodic paralysis (hypokalaemic, hyperkalaemic or normokalaemic), and cardiac manifestations (long QT, ventricular arrhythmia, bigeminy, torsade de pointes).

The dysmorphic features of Andersen' patients range from subtle to severe, affecting craniofacial features (hypertelorism, micrognathia, low-set ears, broad-base nose and high arched or cleft palate) and the trunk and limbs (short stature, scoliosis, syndactyly, and clinodactily) (Andersen *et al.*, 1971; Tawil *et al.*, 1994; Sansone *et al.*, 1997; Tristani-Firouzi *et al.*, 2002).

Functional analysis of mutations associated with ATS confirmed the role of Kir2.1 in skeletal muscle and cardiac tissues.

### 1.4.1. Molecular genetics of ATS

ATS is inherited in an autosomal dominant manner. Functional analyses have revealed that most of the KCNJ2 gene mutations cause loss of function and dominant negative suppression of the Kir2.1 channel, thereby abolishing or reducing the inward rectifier K<sup>+</sup> channel current (I<sub>K1</sub>) (Sung *et al.*, 2006). The skeletal muscle and cardiac symptoms are accounted for the most cases through a dominant negative effect of mutations on K<sup>+</sup> channel current, resulting in prolonged depolarization of the AP. The dominant negative nature of ATS mutations (Guo and Lu, 2003) has been well-described, whereby heterologous expression of WT Kir2.1 with any number of mutant Kir2.1 subunits resulted in a loss of current (Tawil *et al.*, 1994; Melnyk *et al.*, 2002; Yoon *et al.*, 2006).

Multiple missense mutations in Kir2.1 have been identified in patients with ATS, affecting channel function. Many are believed to disrupt channel regulation by the PIP2 (Lopes *et al.*, 2002; Donaldson *et al.*, 2003). Others have been shown to alter gating (Chen *et al.*, 2002).

In this study I characterized electrophysiologically mutations found in the KCNJ2 gene. These pathogenetic mutations occurred in patients with clinical features associated with Andersen-Tawil syndrome, such as cardiac arrhythmias, periodic paralysis and dysmorphic features. I investigated the biophysical properties of Kir2.1 mutations and tried to understand the mechanism behind their dysfunction linked to the disease.

Some of the results have been reported at the Annual Meeting of the Biophysical Society (Long Beach, California, USA, 2005), EC Coupling Midterm Meeting (Ulm, 2005), Annual Congress of the German Physiological Society, (Göttingen, 2005; München, 2006). A manuscript to publish the findings is in preparation.

## 2 AIM OF THE STUDY

Mutations in KCNJ2, which encodes the  $\alpha$ -subunit of Kir2.1, an inwardly-rectifying potassium channel, have been identified as the genetic defects underlying the clinical phenotype of Andersen-Tawil syndrome (ATS) or rare cases of atrial fibrillation. ATS is an autosomal dominant disease characterized by ventricular arrhythmias, periodic paralysis and dysmorphic features. It occurs when the mutation causes a loss of channel function.

The purpose of the present study was to investigate the biophysical properties of WT Kir2.1 and novel mutations in the KCNJ2 gene (D78G, R82W, V93I and G215R). Therefore I needed to perform the following experiments:

- 1) The **D78G** mutation in Kir2.1 occurs in a highly conserved but functionally undetermined region within the N-terminus immediately adjacent to the M1 segment. Additionally, crystallographic studies located this residue within the slide helix of the channel segment that has been suggested to play a role in the gating process. Therefore, I wanted to perform whole-cell patch clamp experiments in order to characterize this mutant channel. These experiments will answer the question, whether the homo- or heterogenous expression of this mutant channel can influence whole-cell current.
- 2) The substitution of tryptophan for arginine **R82W** is also located on the intracellular side of the channel in the cytoplasmic N-terminus. This region could be involved in the formation of a long and wide intracellular pore vestibule that protrudes into the cytoplasm (Lu *et al.*, 1994). Mutations occurring in this N-terminal region may disrupt the correct insertion of the M1 segment into the membrane (Umigai *et al.*, 2003). Therefore I wanted to investigate whether the R82W mutant channel has a different ion permeation in the pore region compared to WT channels, and how extracellularly applied  $Ba^{2+}$ , which is a blocker of the inward-rectifier channels (Alagem *et al.*, 2001), blocks R82W mutant channels.
- 3) The C-terminal domain is important for Kir2.1 channel assembly (Tinker *et al.*, 1996). The **G215** mutation is located in this channel region. Therefore, I wanted to investigate the subcellular distribution of the G215R mutant Kir2.1 channels and compare it with published data on G215D mutant previously described by Hosaka *et al.* (2003). Therefore, I wanted to perform confocal laser microscopy experiments with tagged, fluorescent-labelled G215R mutant and WT Kir2.1

channels. Additionally, I wanted to investigate the electrophysiological consequences of G215 substitutions to arginine and aspartic acid.

- 4) Individuals presenting with atrial tachycardia (AT) showed an amino acid substitution in the outer helix of the M1 segment of the Kir2.1 channel (**V93I**). This mutation occurs in a highly conserved sequence among Kir channels. Therefore, I wanted to see how this mutation changed channel function.

This study provides new knowledge on the biophysical defects caused by Kir2.1 mutations occurring in ATS or AT

### 3 MATERIALS AND METHODS

#### 3.1 Molecular biology methods

##### 3.1.1 Solutions and chemicals for molecular biology methods

All chemicals of quality „pro analysis“ were obtained from the following companies (Germany): Amersham Pharmacia (Braunschweig), Bio-Rad (München), Fluka Chemika (Neu-Ulm), Invitrogen (Karlsruhe), Life Technologies (Eggenstein), MBI Fermentas (St. Leon), Merck (Darmstadt), NewEngland BioLabs (Frankfurt), Qiagen (Hilden), PeqLab Biotechnology (Erlangen), Roche (Mannheim), Serva (Heidelberg), Sigma Aldrich (Deisenhofen), and Stratagene (Heidelberg).

Solution sterilisation was performed by autoclaving the solutions for 20 min at 121°C, and a pressure of 1.2 bar, or by sterile filtration using minifilters from Millipore (Molsheim, France), with a pore diameter of 0.22 µm.

**Table 1. Solutions, chemicals and antibiotics used in the molecular biology methods**

<b>Solution</b>	<b>Details/Preparation</b>
ampiciline stock solution	100 mg/ml; sterile filtrated
kanamycin stock solution	100 mg/ml; sterile filtrated
DNA standard ladder	1 Kb-standard
DNA ladder buffer	15 % ficoll, 0.1% bromphenolblue
dNTP-Mix	2.5 mM dATP, 2.5 mM dCTP, 2.5 mM dGTP, 2.5 mM dTTP, in H <sub>2</sub> O
EDTA stock solution	0.5 M ethylene diamine sodium tetraacetate (pH 8.0), in H <sub>2</sub> O
ethidium bromide	10 mg/ml
isopropanol/ potassium acetate solution	1 Vol. (5 M) potassium acetate, 2 Vol. H <sub>2</sub> O, 22 Vol. isopropanol (88 %)
potassium acetate	5 M
potassium acetate/Acetic acid solution	4 Vol. (5 M) potassium acetate, 1 Vol. 10 M acetic acid (57 %)
LB medium	1 % peptone, 0.5 % yeast extract, 1 % NaCl, in H <sub>2</sub> O, pH 7.5; autoclaved

LB Medium – Agar	LB medium with 2 % agar; autoclaved
2YT medium	1.6 % peptone, 1 % yeast extract, 0.5 % NaCl, in H <sub>2</sub> O, pH 7.5; autoclaved
Solution I	50 mM glucose, 10 mM Tris, 1 mM EDTA
Solution II	0.2 N NaOH, 1 % SDS
STE solution	100 mM NaCl, 10 mM Tris, 1 mM EDTA
TBE buffer	89 mM Tris, 89 mM Boric acid, 2 mM EDTA
TE buffer	10 mM Tris, 1 mM EDTA, pH 7.5
BmtI, NheI, XhoI	restriction enzymes

### 3.1.2 DNA Clones

The WT and mutants KCNJ2 were a kind gift of PD Dr. Karin Jurkat-Rott (Ulm University, Germany) who found four novel mutations (D78G, R82W, V93I and, G215R) and one already described mutation (G215D) in 132 individuals. In the following section I will shortly describe the clinical features of the patients from ATS family obtained by PD Dr. Karin Jurkat-Rott:

Seven patients from 3 small ATS families and one family with periodic paralysis and atrial fibrillation (AF) underwent neurological and electrocardiogram (ECG) examination. One patient gave informed written consent to a quadriceps muscle biopsy. For comparison, three control muscle specimens were obtained from individuals who had undergone muscle biopsy for exclusion of malignant hyperthermia susceptibility. All affected genotyped individuals harboured pathogenic mutations. The carrier of the D78G mutation (male) had hypokalemic periodic paralysis (HypoPP) (onset at age 8), cardiac arrhythmias (onset at age 17), and dysmorphic features. Both individuals carrying R82W were males aged 74 and 34. While the older patient had frequent ventricular extrasystoles, often as bigeminy or couplets, permanent distal leg weakness, and scoliosis, the younger had hypertelorism, short stature and low-set ears, and showed with periodic hypokalemic weakness only in association with hyperthyroidism. Individuals carrying V93I mutation have not yet had an episode of AF. The male patient (69 years of age) had asymptomatic runs of atrial tachycardias (AT) in Holter ECGs. The P-wave in his ECG was slightly prolonged but there was no echocardiographic sign of structural alterations in the atria. The ECG of his daughter (40 years of age) revealed no pathologies. The QTc-times of both patients were normal.

Carriers showed a short QT syndrome with a narrow and peaked T-wave, i.e. affecting ventricular repolarization. In this V93I family, QT-time and T-wave were normal.

In a single ATS individual of 22 years of age a *de novo* G215D mutation was identified in the KCNJ2 gene. The individual (male) showed a short stature, ocular hypertelorism and clinodactily. Since the age of 3 years, he had experienced periodic attacks of generalized, proximally pronounced muscle weakness associated with hyperkalemia. Arrhythmias or long-QT was not observed in resting or Holter ECGs. Two female patients, (aged 38 and 11) carried the G215R mutation with disease onset at age 9-10. Prominent in both patients were monthly occurring attacks of HypoPP lasting for days. Additionally, the older patient had permanent weakness and vacuolar myopathy. Dysmorphic features in both were ocular hypertelorism, hypotrophic mandible, low set ears and clinodactily. The older patient carrying the G215R mutation had an extremely severe ATS phenotype concerning the highly symptomatic ventricular arrhythmias (ventricular tachycardias leading to syncope) with characteristic ECG features, frequent paralytic episodes and dysmorphia.

This study by PD Dr. Karin Jurkat-Rott was approved by the local ethics committee at Ulm University. Blood from patients was taken with their informed written consent. The products were cleaned using Qiagen PCR purification kits, and both strands were sequenced using a Big Dye Terminator sequencing kit (ABI Applied Biosystems, Foster City, CA). Any sequence variants identified were sought in other family members by direct DNA sequencing. Screening of 80 control samples was performed by direct DNA sequencing. DNA sequencing identified five heterozygous single nucleotide substitutions in KCNJ2: c.233A→G (D78G), c.244C→T (R82W), c.277G→A (V93I), c.643G→C (G215R) and c.644G→C (G215D). Paternity testing was performed by genotyping using 14 highly polymorphic fluorescent microsatellite markers on 10 different autosomes.

The WT (GenBank Accession AF153819) and mutants KCNJ2 were cloned into a pcDNA3.1 (+) vector, the fluorescent labelled-tagged WT and G215R and were cloned into a pEGEP vector, respectively and were used in this form for transfection into mammalian COS-7 cells.

### **3.1.3 The transformation procedure**

The DNA plasmids were introduced through transformation and amplified into *E. coli*. For transformation I used competent cells obtained through the CaCl<sub>2</sub> method (Mandel and

Higa, 1970). Shortly, the competent cells were obtained as follows: One colony of XL 1-Blue *E. coli* was grown over night in LB medium at 37°C and at 200 rpm. From this over night culture, 1/50 Vol. was recultured in LB medium at 37°C and shaken (200 rpm) until it reached an OD<sub>600</sub> = 0.3 to 0.5. This bacterial culture was incubated on ice for 20 minutes, and then centrifuged at 3000 x g, 4°C. The pellet was resuspended in ice cold 0.1 M CaCl<sub>2</sub> (half of the volume in which the bacteria reached the OD<sub>600</sub> of 0.3 to 0.5), incubated on ice for 30 minutes, and recentrifuged for 5 minutes (3000 x g, and 4°C). The pellet was resuspended in 1/10 of the initial volume of ice cold 0.1 M CaCl<sub>2</sub>, and the bacterial suspension was left at 4°C for 36 hours. After this incubation interval I obtained competent bacterial cells ready for transformation.

For transformation I incubated approximate 100 ng of plasmid DNA together with the competent cells prepared as previously described (the volume of the transformed plasmid was never higher than 1/20 from the total volume) on ice for 1 hour. A heat shock of 45 sec at 42°C, in a water bath, allowed the plasmids to enter the bacterial cells. After 10 min of incubation on ice, 300 µl of LB or 2YT medium was added and, for a better efficiency of the transformation, the suspension was shaken (500 rpm) 1h, at 37°C. Finally, 100-300 µl of this suspension was plated on agar plates containing antibiotics, and incubated over night at 37°C. The single colonies obtained next day were used for plasmid DNA isolation and purification.

### **3.1.4 Plasmid DNA isolation and purification**

For the plasmid DNA isolation and purification I used the miniprep-isolation without phenol extraction described by Feliciello *et al.* (1993). The single colonies obtained following the transformation, were shaken overnight at 37°C in 5 ml LB or 2YT medium (2YT medium was used when PCR DNA products were amplified). Cells were centrifuged 5 min at 1000 g or 2000 rpm at 4°C. The pellet was washed in 500 µl ice cold STE solution (Table 1) and the cells were resuspended. The pellet was then centrifuged at 6000 g for 1 min at 4°C. The pellet was resuspended in 125 µl ice cold Solution I (Table 1), and vortexed. 250 µl fresh Solution II (Table 1) was added and the Eppendorf tubes were inverted 4-5 times. The resulting product was incubated 3-5 min on ice. 375 µl ice-cold Potassium Acetate/Acetic acid solution (Table 1) was added, and the whole content agitated. The resulting product was incubated 5-10 min on ice and then centrifuged at 12000 g for 5 min at 4°C. 700 µl were transferred in a new Eppendorf tube. The following procedures were performed at room temperature. For precipitation 350 µl isopropanol

(Table 1) was added and inverted 6-7 times. The probe was then centrifuged at 12000 g for 5 min and the supernatant was removed. The solution left in the Eppendorf tubes was centrifuged for 30 sec and removed with a pipette. 125  $\mu$ l TE together with 10  $\mu$ g/ml Rnase (Table 1) were added to the pellet and incubated for 15 min at room temperature. The pellet was treated with 150  $\mu$ l isopropanol/potassium acetate solution (Table 1), vortexed and after 10 min at room temperature incubation was centrifuged at 12000 g for 5 min. The supernatant was immediately removed. The pellet was dried and dissolved in 50  $\mu$ l TE buffer. The plasmids were stored at  $-20^{\circ}\text{C}$  or  $-80^{\circ}\text{C}$ .

### 3.2 Cell culture

#### 3.2.1 Solutions and chemicals

All the solutions and chemicals (see Table 2) were bought from Invitrogen (Karlsruhe, Germany), and the cell culture materials were provided from Dow Corning (Seneffe, Belgium).

**Table 2. Solutions and chemicals used to culture the cells and prepare them for the electrophysiological measurements.**

Solution	Details/Preparation
DMEM medium	Dulbecco's modified Eagle's medium
MEM medium	Minimum Essential Medium
FBS	Fetal bovine serum
PBS	Phosphate buffered saline without calcium, magnesium, and sodium bicarbonate
Polylysine	0.5 mg/ml
Sylgard	Sylicon-Elastomer, heat polymerized

#### 3.2.2 Cell culture of COS-7 celline

In my experiments I used COS-7 (African green monkey kidney) cells and their correspondent culture medium. The COS-7 cell line was purchased from the DSMZ (Deutsche Sammlung von Mikroorganismen und Zellkulturen GmbH, Braunschweig, Germany). Cells were maintained in culture medium Dulbecco's modified Eagle's medium with high glucose (DMEM with Earle's salts, Cat. No. 41966-029, Invitrogen, Carlsbad,

CA) with 10 % heat-inactivated FBS (PAA Laboratories GmbH, Coelbe, Germany) and cultured at 37°C and 10 % CO<sub>2</sub> in a humidified incubator (Kendro Laboratory Products GmbH, Hanau, Germany). The confluent cells (3-4 days old) were washed with PBS, trypsinized, resuspended in new medium, and splitted in new flasks, in a dilution of 1: 10 or 1: 5. Cells were measured 48-72 hours after transfection. The measuring chambers consisted of Teflon rings (2 cm in diameter) glued with Sylgard (Table 2) to glass cover-slips. Trypsinized transiently transfected COS-7 cells were plated on polylysine (Table 2) coated glass cover-slips 10 minutes before measurements.

### **3.2.3 Transfection**

To test whether the mutant Kir2.1 channel subunits were able to form functional homo- or heteromultimeric channels I transfected each mutant in COS-7 cells alone or together with the WT Kir2.1. The pcDNA3.1(+) vector containing the entire coding sequence of WT or mutant Kir2.1 channels containing the coding sequence of WT Kir2.1, or mutant channels were co-transfected together with a GFP expressing construct into COS-7 cells using the FuGene6 transfection reagent (Roche Molecular Biochemicals, Germany).

The COS-7 cells were plated on Petri dishes 1 day prior to transfection. The transfection was performed when cell density reached 50 - 70% confluency. Shortly the transfection was performed as follows: in one sterile tube with 94-97 µl culture medium without FBS were added 3-6 µl FuGene6 transfection reagent; after 5 minutes at room temperature, a mixture of 1 µg plasmid DNA containing the coding sequences of the channel (WT or mutant KCNJ2) and 0.5 µg pEGFP vector were added to the FuGene6 containing solution. After 15 minutes, the transfection mix was added directly to the cells whose culture medium was removed. After 2 minutes, the transfected cells were supplemented with FBS containing culture medium and kept in the incubator. The same transfection procedure was used for the confocal microscopy measurements. Two days after transfection sufficient protein was expressed for electrophysiological measurements and confocal microscopy measurements. Co-transfection was made with 0.5 µg of WT and 0.5 µg of mutant together with 0.5 µg of pEGFP DNA (BD Biosciences Clontech, Palo Alto, CA).

### **3.3 Electrophysiology**

#### **3.3.1 Solutions and chemicals for electrophysiology**

All chemicals of quality, “pro analysis” were obtained from the following companies in Germany: Fluka Chemika GmbH, Neu-Ulm (HEPES), Carl-Roth Chemika GmbH+Co, Karlsruhe (CaCl<sub>2</sub>), Merck KGaA, Darmstadt (NaCl), Sigma Aldrich Chemie GmbH, Steinheim (EGTA and potassium aspartate) and Fluka Chemika GmbH, Buchs (KCl, ATP and MgCl<sub>2</sub>).

Cells were measured in normal mammalian Ringer’s solution, low K<sup>+</sup><sub>out</sub>, containing (in mM): 160 NaCl, 4.5 KCl, 2 CaCl<sub>2</sub>, 1 MgCl<sub>2</sub>, and 10 HEPES, or high K<sup>+</sup><sub>out</sub> where NaCl was replaced by KCl (final [K<sup>+</sup>]<sub>out</sub> 164.5 mM). The pH was adjusted to 7.4 with NaOH or KOH, respectively, with an osmolarity of 290 to 320 mOsM. A simple syringe-driven perfusion system was used to exchange the bath solution in the recording chamber. The internal pipette solution contained in mM: 160 potassium aspartate, 2 MgCl<sub>2</sub>, 0.1 CaCl<sub>2</sub>, 1.1 EGTA, 10 HEPES and 0.5 ATP. The pH was adjusted to 7.2 with KOH with an osmolarity of 290 to 320 mOsM.

#### **3.3.2 Electrophysiological recordings and data analysis**

All the experiments were carried out at room temperature (21–25°C) using the whole-cell recording mode of the patch-clamp technique (Hamill *et al.*, 1981; Rauer and Grissmer, 1996). Electrodes were pulled from glass capillaries (Science Products, Hofheim, Germany) in three stages and fire-polished to a resistance measured in the bath of 2.5 to 5 MΩ. Membrane currents were recorded (48-72 h after transfection) with an EPC-9 patch-clamp amplifier (HEKA elektronik, Lambrecht, Germany) connected to a Macintosh computer running Pulse/Pulse Fit Ver. 8.40 data acquisition and analysis software (HEKA elektronik, Lambrecht, Germany). All currents were filtered by a 2.9-kHz Bessel filter and recorded with a sampling frequency of 2.00 kHz. Capacitative and leakage currents were subtracted (unless otherwise mentioned), and series resistance compensation (80%) was used for currents exceeding 2 nA. Transfected and co-transfected cells (1 μg of WT KCNJ2 and/or 1 μg of mutant KCNJ2) were identified by GFP fluorescence using fluorescence microscopy on the stage of an inverted microscope AXIOVERT<sup>®</sup> 100 (Carl Zeiss Jena GmbH, Germany). Two days after transfection cells were measured in order to compare the expression of the mutant KCNJ2 channels compared with the WT channels. In

parallel the co-expression in a 1:1 ratio of the WT channels together with each mutant channel was investigated. For data analysis I considered measurements of a number of  $n$  cells from the same day expressing the WT channels alone, the respective mutant KCNJ2 channels alone and their co-expression. Membrane currents were elicited by 200 ms pulses applied in 10 mV increments, every 5 s, to potentials ranging from -120 to +40 mV, from a holding potential of -60 mV for low  $[K^+]_{out}$  and 0 mV for high  $[K^+]_{out}$ , respectively. The peak currents were converted into corresponding conductance's by dividing the peak current amplitude at -120 mV with the driving force for  $K^+$  ( $E - E_K$ , with  $E_K = -80$  mV in 4.5 mM  $[K^+]_{out}$  and with  $E_K = 0$  mV in 164.5 mM  $[K^+]_{out}$ , respectively).

Data were given as mean  $\pm$  S.E.M. (with  $n$  the number of observations). For electrophysiological experiments, the statistical analysis was performed using ANOVA and Student's  $t$ -test,  $P < 0.05$  was considered significantly different. Data analyses were performed using Igor Pro 3.1 (WaveMetrics, Lake Oswego, OR) and ORIGIN 6.0 software package (MicroCal Inc., Northampton, MA).

### ***3.4 Confocal microscopy experiments***

All experiments were recorded and analysed using the Radiance 2000 Confocal Scanning Microscope produced by Byroad Cell Science Division (Hemel Hempstead, UK) adapted to an Eclipse TE300 inverted microscope (Nikon Corporation, Tokyo, Japan). Furthermore, a Plane 60 x oil objective was used and fluorescence was excited with the 488 nm wavelength of the Argon laser and emission was measured using a HQ530/60 filter.

### ***3.5 Structural modelling***

Structural models of Kir2.1 were constructed by comparative modelling using DeepView/Swiss-PdbViewer v3.7 program (Guex, 1995-2001). I used the Data Bank accession codes: 1P7B (KirBac1.1) and 1UF (Kir2.1) as templates.

## 4 RESULTS

In the first part of my results I attempted to characterize the biophysical properties of WT and novel mutations in the KCNJ2 gene (D78G, R82W, V93I and, G215R) associated with Andersen-Tawil syndrome and/or atrial fibrillation. Since the KCNJ2 gene encodes the inward-rectifier Kir2.1 potassium channel I investigated the electrophysiological function of these mutant channels and their influence on the WT Kir2.1 channel. I performed whole-cell patch-clamp experiments, measured inward currents in mammalian expression systems after transfection with only the WT or mutant Kir2.1 channels or in combination, and investigated the Ba<sup>2+</sup> and K<sup>+</sup> sensitivity of the mutant Kir2.1 channels.

Additionally, I used a confocal laser microscope to investigate the subcellular distribution of the G215R mutant Kir2.1 channels.

### *4.1 Overview of the biophysical characterization of novel Kir2.1 mutations associated with ATS*

In order to assess the functional expression of the novel mutations identified in the KCNJ2 gene, I used the whole-cell mode of the patch-clamp technique. To characterize their electrophysiological properties I transiently transfected COS-7 cells with cDNA coding for WT or mutant (D78G, R82W, V93I and G215R) Kir2.1 channels (1 µg/ transfection) and compared the resulting current (Fig. 4). Current traces were elicited by 200 ms pulses ranging from -120 to +40 mV in 20 mV steps, repeated every 5 second, at a holding potential of -60 mV.

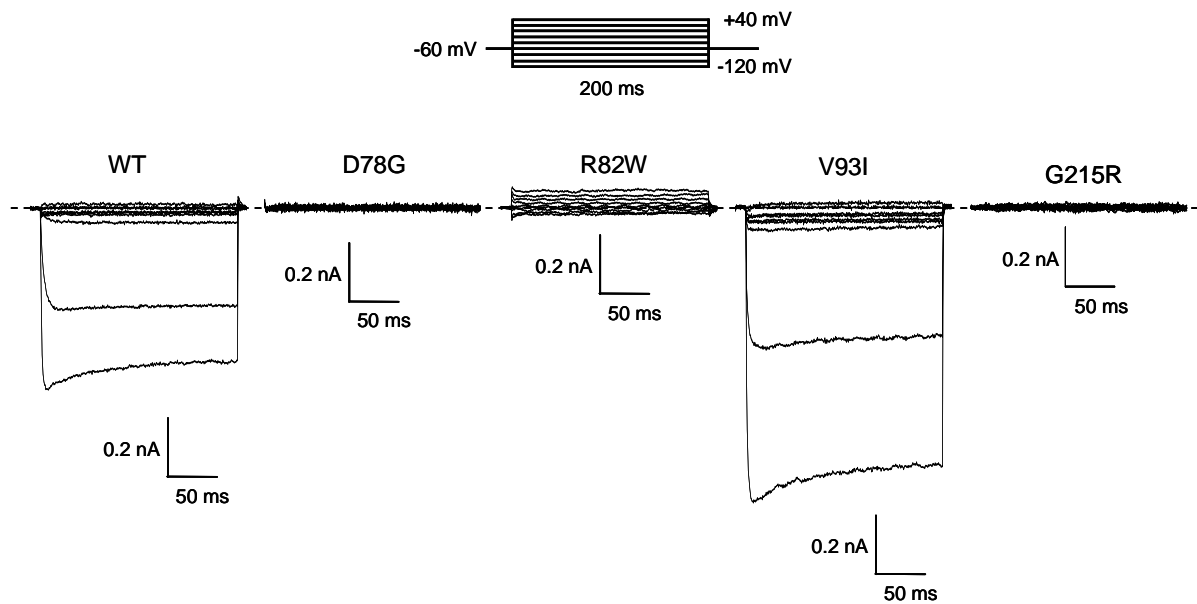


**Fig. 4. Functional characterization of novel ATS-associated mutations in KCNJ2.** Whole-cell currents measured in COS-7 cells transfected with only WT or D78G, R82W, V93I, or G215R mutant Kir2.1 channels. Cells were held at -60 mV holding potential and currents were elicited by stepping to various test potentials (see inset from -120 to +40 mV) for 200 ms duration in 20 mV steps, repeated every 5 seconds.

WT Kir2.1 channels open at hyperpolarized potentials. Control currents through WT Kir2.1 channels are shown in Fig. 4 (column 1). Holding the membrane potential at -60 mV I applied the first pulse at -120 mV and observed large inward current (Fig. 4, column 1) of more than 500 pA amplitude. Pulsing to less negative potentials resulted in reduced inward currents with hardly any outward currents (< 50 pA). Therefore the transfection of WT Kir2.1 resulted in much larger inward than outward current, i.e. strong inward rectification consistent with Kir2.1 channel activity (Leonoudakis *et al.*, 2004). Cells transfected with the D78G mutant Kir2.1 channels lack this inward  $K^+$  current (Fig. 4, column 2). Cells transfected with the R82W mutant Kir2.1 channels showed inward current with amplitudes of about 50-100 pA (Fig. 4, column 3) and outward current of about 100 pA. In addition, cells transfected with the V93I mutant Kir2.1 channels (Fig. 4, column 4) showed larger current amplitudes than those cells transfected with WT Kir2.1. Cells transfected with the G215R mutant Kir2.1 channels did not show any current (Fig. 4, column 5).

My experiments demonstrated that homomeric channels of the D78G (Fig. 4, column 2) or G215R (Fig. 4, column 5) mutants did not show any current, whereas the R82W (Fig. 4, column 3) showed little and the V93I (Fig. 4, column 4) mutants did show large currents indicating the formation of functional homomeric channels.

As a followup of these initial experiments I wanted to answer the question whether the transfection of the mutant channels in combination with the WT channels can influence current through WT Kir2.1 channels.

#### 4.2 Co-transfection experiments with WT and D78G mutant Kir2.1 channels

In electrophysiological measurements, the D78G mutant Kir2.1 transfected alone (Fig. 4, column 2) did not show any current. Therefore I wanted to test whether the D78G mutant Kir2.1 subunits were able to influence current through WT Kir2.1 channels and consequentially co-transfected cells with cDNA coding for WT and D78G mutant Kir2.1 channels (Fig. 5).

Current traces were elicited with the same protocol as described for Fig. 4 and inward currents were compared when cells were transfected with only the WT or D78G mutant Kir2.1 channels or in combination.

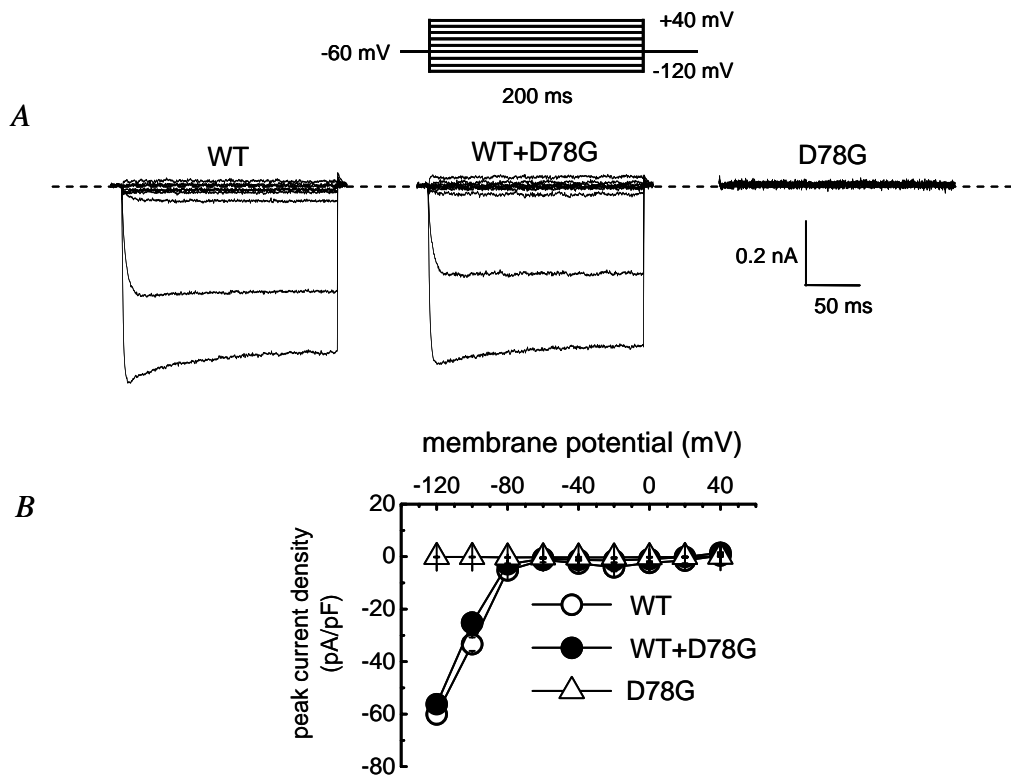


**Fig. 5. Functional characterization of D78G mutant Kir2.1 channels co-expressed with WT Kir2.1 channels.** A Whole-cell currents measured in COS-7 cells transfected with WT (*left*), WT+D78G mutant (*middle*), and D78G mutant alone (*right*). Cells were held at -60 mV holding potential and currents were elicited as described in legend to Fig. 4. B Peak currents from records shown in A and similar experiments were divided by the respective cell capacitance and the peak current density was plotted against the applied membrane potential. Values are mean  $\pm$  S.E.M. (n= 2-6). S.E.M. is shown as bars when it exceeds the size of the symbol.

Current through WT Kir2.1 (Fig. 5 A, *left*) showed strong inward rectification, as already shown and described in Fig. 4 and no currents were observed in cells transfected with only D78G mutant Kir2.1 channels. Several independent co-transfection experiments (WT+ D78G) showed similar results. Peak currents from records shown in Fig. 5 A and similar experiments were divided by the respective cell capacitance and the obtained peak current density was plotted against the applied membrane potential (Fig. 5 B). At -120 mV the peak current density was  $-60\pm 3.6$  pA/pF for WT,  $-56.19\pm 1.9$  pA/pF for WT+ D78G and  $-0.14\pm 0.12$  pA/pF for the D78G mutant channels. Co-transfected cells (Fig. 5 A, *middle* and B filled circles) showed similar inward currents to those recorded in cells transfected with only WT Kir2.1 channels. This indicates the possibility of mutant subunits to co-assemble with WT subunits and form heterotetrameric channels.

In contrast to the D78G mutant, the R82W mutant Kir2.1 channels did show small inward currents when transfected alone (Fig. 4, column 3). Therefore I wanted to see how the transfection of R82W mutant channels in combination with WT channels will influence current through WT Kir2.1 channels.

### ***4.3 Properties of the R82W mutant Kir2.1 channels***

#### **4.3.1 Co-transfection experiments of the R82W mutant Kir2.1 channels**

The transfection of the R82W mutant Kir2.1 channels alone resulted in little inward current as already shown and described in Fig. 4 (column 2). To test whether the transfection of the R82W mutant channels can influence current through WT Kir2.1 channels, I co-transfected cells with cDNA coding for WT and for R82W mutant Kir2.1 channels (Fig. 6). Current traces were elicited with the same protocol as described for Fig. 4 and inward currents were compared when cells were transfected with only WT or R82W mutant Kir2.1 channels or in combination. Current through WT Kir2.1 channels (Fig. 6 A, *left*) showed strong inward rectification, as already shown and described in Fig. 4. The co-transfection of R82W mutant and WT Kir2.1 channels showed that the inward current was reduced only a little compared to homotetrameric WT Kir2.1 channels (Fig. 6 A, *middle*). Interestingly, when R82W mutant Kir2.1 channels are expressed alone the inward current is drastically reduced compared to the current through WT Kir2.1 channels (Fig. 6 A, *right*).

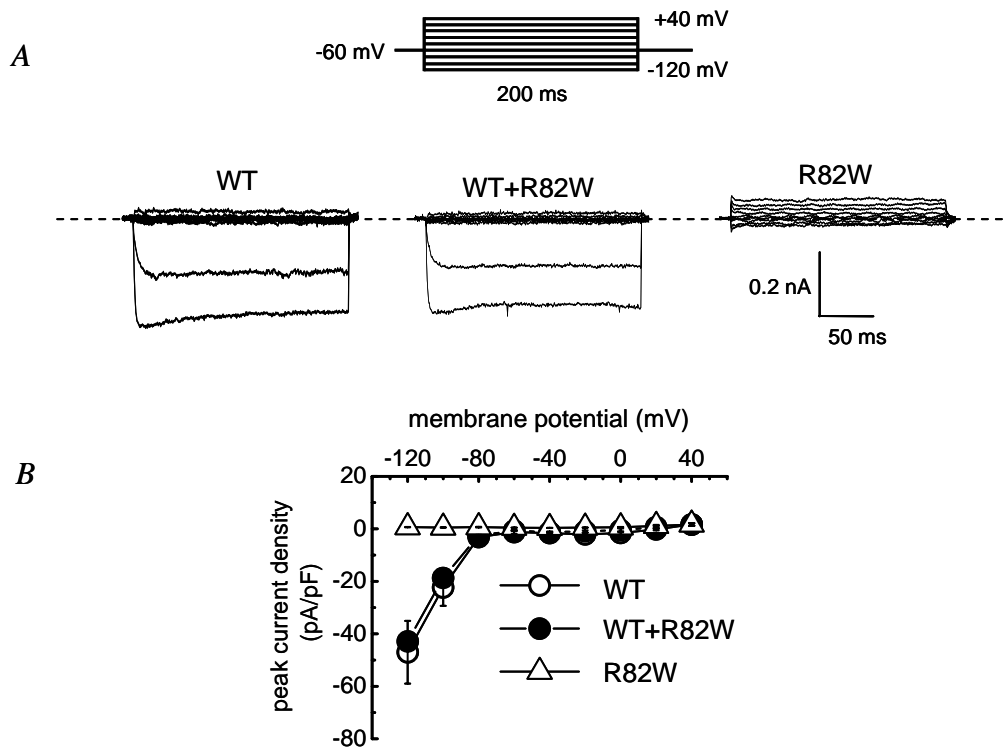


**Fig. 6. Functional characterization of R82W mutant Kir2.1 channels co-expressed with WT Kir2.1 channels.** *A* Whole-cell currents measured in COS-7 cells transfected with WT (*left*), WT+R82W mutant (*middle*), and R82W mutant alone (*right*). Cells were held at -60 mV holding potential and currents were elicited as described in legend to Fig. 4. *B* Peak currents from records shown in *A* and similar experiments were divided by the respective cell capacitance and the peak current density was plotted against the applied membrane potential. Values are mean  $\pm$  S.E.M. ( $n = 2-6$ ). S.E.M. is shown as bars when it exceeds the size of the symbol.

Several independent co-transfection experiments (WT+R82W) showed similar results. Peak currents from records shown in Fig. 6 *A* and similar experiments were divided by the respective cell capacitance and the obtained peak current density was plotted against the applied membrane potential (Fig. 6 *B*). At -120 mV the peak current density was  $-46.9 \pm 11$  pA/pF for WT,  $-42.8 \pm 3.12$  pA/pF for WT+R82W and  $-0.62 \pm 0.09$  pA/pF for R82W mutant channels.

Current through inward-rectifier  $K^+$  current strongly depend on external potassium  $[K^+]_{out}$ . An increase in the  $[K^+]_{out}$  usually leads to an increased in inward current. Since the R82W mutant Kir2.1 channel did show a small current in 4.5 mM  $[K^+]_{out}$  the question was whether this current would increase in higher  $[K^+]_{out}$ . To answer this question I performed experiments with 164.5 mM  $[K^+]_{out}$  instead of 4.5 mM  $[K^+]_{out}$ .

### 4.3.2 Pharmacological characterization of the R82W mutant Kir2.1 channel

Currents in cells transfected with R82W mutant Kir2.1 channels were measured in 4.5 and 164.5 mM  $[K^+]_{out}$  and were compared with currents through WT Kir2.1 measured under the same conditions. Cells were held at -60 mV holding potential in 4.5 mM  $[K^+]_{out}$  (Fig. 7 A and D) and at 0 mV in 164.5 mM  $[K^+]_{out}$  (Fig. 7 B and E) and currents were elicited by stepping to various test potentials (from -120 to +40 mV) for 200 ms duration in 20 mV steps repeated every 5 seconds. Current through WT Kir2.1 showed strong inward rectification (Fig. 7 A), as already described and shown in Fig. 4, and increased in 164.5 mM  $[K^+]_{out}$  as expected for inward-rectifier currents (Fig 7 B). Transfection of R82W mutant Kir2.1 channels resulted in small inward currents at low  $[K^+]_{out}$  (4.5 mM) (Fig. 7 D). This small inward current through homomeric R82W mutant Kir2.1 channels increased with high  $[K^+]_{out}$  (164.5 mM) in a manner similar to current through homomeric WT Kir2.1 channels (Fig. 7 B and E). However, R82W mutant Kir2.1 channels showed a difference in the time course of inward current activation compared to WT channels (Fig. 7 E). WT channels activated rapidly while R82W channels activated slowly. For example, current through R82W mutant channels took about 50 ms at -120 mV to reach peak inward current while current through WT Kir2.1 channels showed an instantaneous current activation. Peak currents from records shown in (A, B, D and E) and similar experiments were plotted against the applied membrane potential (Fig. 7 C and F).

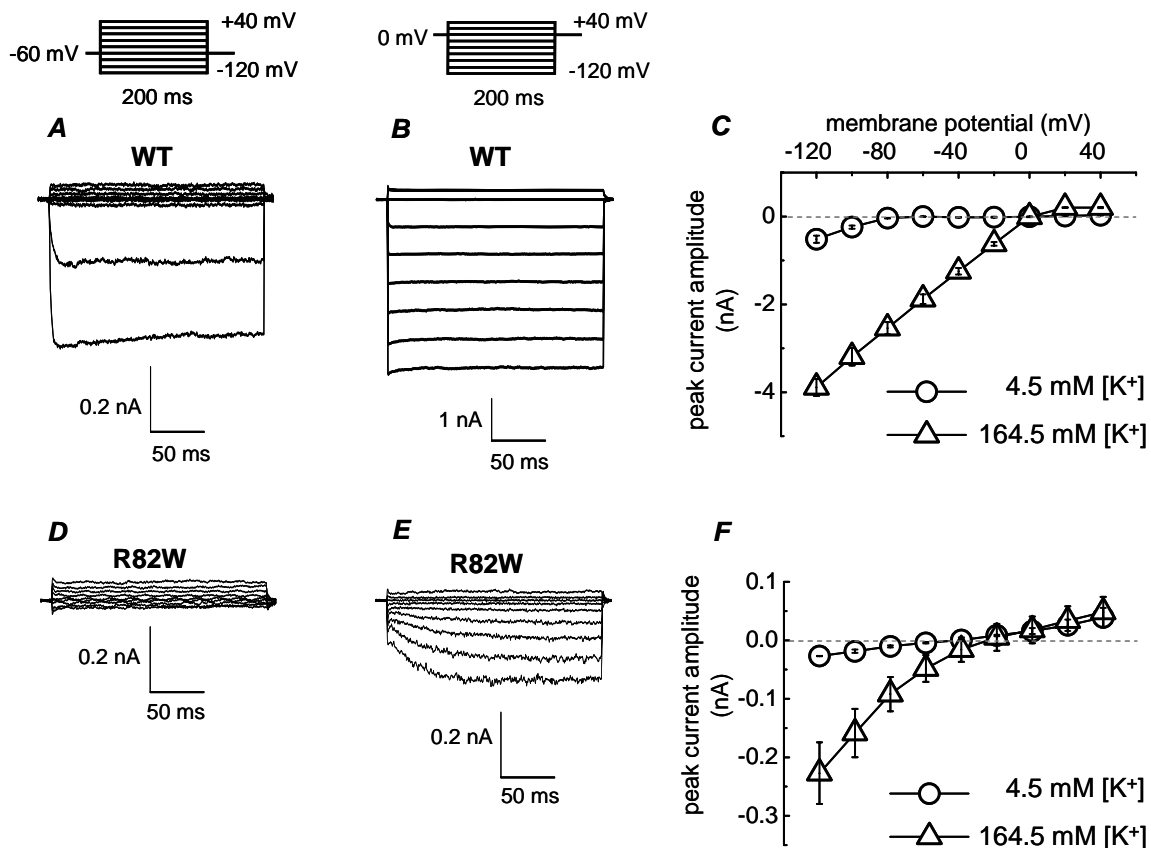


**Fig. 7. Effect of  $[K^+]_{out}$  on WT and R82W mutant Kir2.1 channels.** Whole-cell currents measured in COS-7 cells after transfection with WT Kir2.1 and R82W mutant Kir2.1 channels. Cells were held at -60 mV holding potential in 4.5 mM  $[K^+]_{out}$  (A, D) and at 0 mV in 164.5 mM  $[K^+]_{out}$  (B, E), respectively. Currents were elicited by stepping to various test potentials (from -120 to +40 mV, see insets) for 200 ms duration in 20 mV steps repeated every 5 seconds. C, F. Peak currents from records shown in (A, B, D, E) and similar experiments were plotted against the applied membrane potential. Values are mean  $\pm$  S.E.M. (n= 3-7). S.E.M. is shown as bars when it exceeds the size of the symbol.

Changing  $[K^+]_{out}$  from 4.5 mM (Fig. 7 A) to 164.5 mM (Fig. 7 B) increased the inward current amplitude at -120 mV (Fig. 7 C) by a factor of about 8 for current through WT Kir2.1 channels and by a similar factor for current through R82W mutant Kir2.1 channels (Fig. 7 F). Therefore the  $K^+$  dependence steady-state current through WT and R82W Kir2.1 channels was similar. In addition, the R82W mutant Kir2.1 channels showed a difference in time course of inward current activation compared to WT channels: WT channels activated rapidly while R82W channels activated slowly.

External  $Ba^{2+}$  is known to block current through inward-rectifier Kir2.1 current (Alagem *et al.*, 2001). Since R82W mutant Kir2.1 channels showed small inward current, I wanted to see whether this current could be blocked by external  $Ba^{2+}$ . Moreover, this experiment should allow me to see whether the R82 amino acid substitution induced structural changes

in the channel protein on the outside of the channel and therefore whether the binding site was changed for mutant compared to WT Kir2.1 channels.

#### 4.3.3 Effect of external $Ba^{2+}$ application on WT and R82W mutant Kir2.1 channels

Kir channels show a high sensitivity to external application of  $Ba^{2+}$  in different cell types (Alagem *et al.*, 2001). Therefore I wanted to know whether the R82W mutation in the Kir2.1 channel changed the sensitivity to  $Ba^{2+}$ . To answer this question, I first measured the effect of different external  $[Ba^{2+}]_{out}$  in cells transfected with WT (Fig. 8). Inward currents were measured in high  $[K^+]_{out}$  (164.5 mM, control) plus different  $Ba^{2+}$  concentrations. Current traces were elicited with the same protocol as already described in Fig. 7.

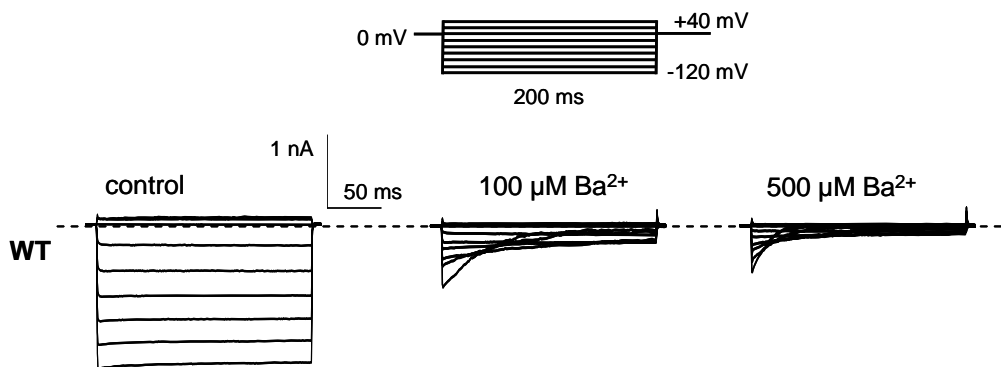


**Fig. 8. Effect of external  $Ba^{2+}$  on current through WT Kir2.1 channels.** Inward currents were measured in 164.5 mM  $[K^+]_{out}$  under control conditions (*left*) and after addition of 100  $\mu M$  (*middle*) and 500  $\mu M$   $Ba^{2+}$  (*right*). Cells were held at a holding potential of 0 mV and currents were elicited as described in legend to Fig. 4.

Control inward currents through WT Kir2.1 channels increased nearly linear with hyperpolarization at potentials more negative than 0 mV (Fig. 8, *left*). At -120 mV the current amplitude of the WT channel was about 2 nA. In the presence of 100  $\mu M$   $Ba^{2+}$  (Fig. 8, *middle*) an initial inward current of about 1 nA (at -120 mV) could be observed at the beginning of the pulse. This initial current declined to about 100 pA (at -120 mV) at the end of the 200 ms pulse. A more pronounced current decline could be observed in the presence of 500  $\mu M$   $Ba^{2+}$  (Fig. 8, *left*) indicating that  $Ba^{2+}$  produced a time-dependent block on the WT Kir2.1 channels (Fig. 8, *middle* and *left*). The time constants of the WT Kir2.1 current decay obtained using a single exponential function (see Fig. 9) were

logarithmically plotted versus voltage. This graph shows that the time dependency of the  $\text{Ba}^{2+}$  block of WT Kir2.1 channels is voltage-dependent, i. e. the more depolarized the membrane potential, the slower is the  $\text{Ba}^{2+}$ -block.

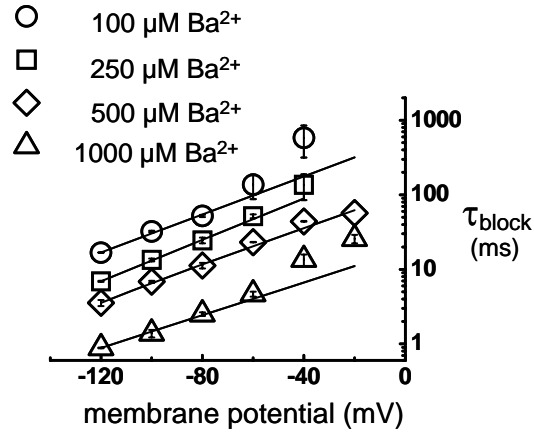


**Fig. 9. Voltage dependence of blocking time constants.** The time constants of the WT Kir2.1 current decay were obtained using a single exponential decaying equation:

$$I = I_0 \exp(-t/\tau_{\text{block}}) + C$$

where,  $I_0$  is the current amplitude at time zero,  $\tau_{\text{block}}$  is the blocking time constant and  $C$  is the steady-state current. The blocking time constants induced by 100, 250, 500 and 1000  $\mu\text{M}$   $\text{Ba}^{2+}$  were obtained from records similar to those shown in Fig. 8 and were plotted against the membrane potential. Data points are mean  $\pm$  S.E.M. ( $n=3$ ). S.E.M. is shown as bars when it exceeds the size of the symbol. The line represents a linear fit assuming that the  $\text{Ba}^{2+}$ -block time constants depend exponentially on the membrane potential. The slope of the line for each  $\text{Ba}^{2+}$  concentration is identical ( $34 \pm 1$  mV).

I analyzed in more detail this voltage-dependence of the time course of the  $[\text{Ba}^{2+}]_{\text{out}}$  block of WT Kir2.1 channels. The  $\text{Ba}^{2+}$  blocking time constants for the WT channels increased exponentially with depolarization (e-fold per  $34 \pm 1$  mV of depolarization). These observations are in agreement with the published data of Alagem *et al.* (2001). They showed that the Kir2.1 channel expressed in oocytes shows highly voltage dependent  $\text{Ba}^{2+}$  block where the ion binds approximately half-way within the membrane electrical field ( $33.9 \pm 1$  mV).

In addition to the quantification of the time course of the  $\text{Ba}^{2+}$  block I also wanted to quantify the effect of  $\text{Ba}^{2+}$  on the steady-state currents through WT Kir2.1 channels. To do so the steady-state currents at the end of the hyperpolarizing pulse (shown in Fig. 8) were

divided by the respective cell capacitance and steady-state current density was plotted against the applied membrane potential. (Fig. 10).

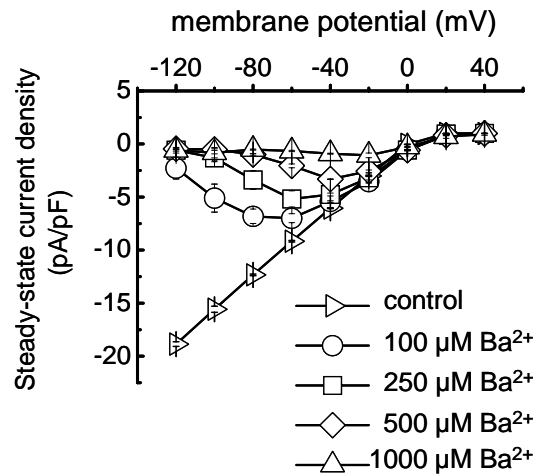


**Fig. 10. Ba<sup>2+</sup> concentration dependence of the steady-state block of WT Kir2.1.**

The steady-state currents from records shown in Fig. 8 and similar experiments were divided by the respective cell capacitance and steady-state current density was plotted against the applied membrane potential. Values are mean  $\pm$  S.E.M. (n=3). S.E.M. is shown as bars when it exceeds the size of the symbol.

Inward currents measured through cells transfected with WT Kir2.1 channels were blocked by 100, 250, 500 and 1000  $\mu\text{M}$  Ba<sup>2+</sup>. Fig. 10 shows that the WT Kir2.1 channel was blocked by Ba<sup>2+</sup> in a dose- and voltage-dependent manner. The block of the inward current by 100  $\mu\text{M}$  Ba<sup>2+</sup> increased at more negative potentials. For example, at 100  $\mu\text{M}$  Ba<sup>2+</sup> the channel was almost completely blocked at -120 mV whereas, at -60 mV only half of the current was blocked.

I quantified in more detail in this voltage-dependent Ba<sup>2+</sup> block of the steady-state current through WT channels (Fig. 12).

Due to the different time course of activation in the WT compared to R82W mutant channels I assumed that Ba<sup>2+</sup> block in R82W channels to be different compared to WT channels. To quantify this difference I measured currents through cells transfected with R82W mutant Kir2.1 and investigated the Ba<sup>2+</sup> block on these channels. Current traces were elicited with the same protocol as already described in Fig. 7.

Control inward currents through R82W mutant Kir2.1 channels increased at potentials more negative than 0 mV (Fig. 11, *left*) but showed no current decline over time compared with the WT Kir2.1 channels. Inward currents through R82W mutant Kir2.1 channels were blocked by 100 (Fig. 11, *middle*) and 200  $\mu\text{M}$  [Ba<sup>2+</sup>] (Fig. 11, *right*).

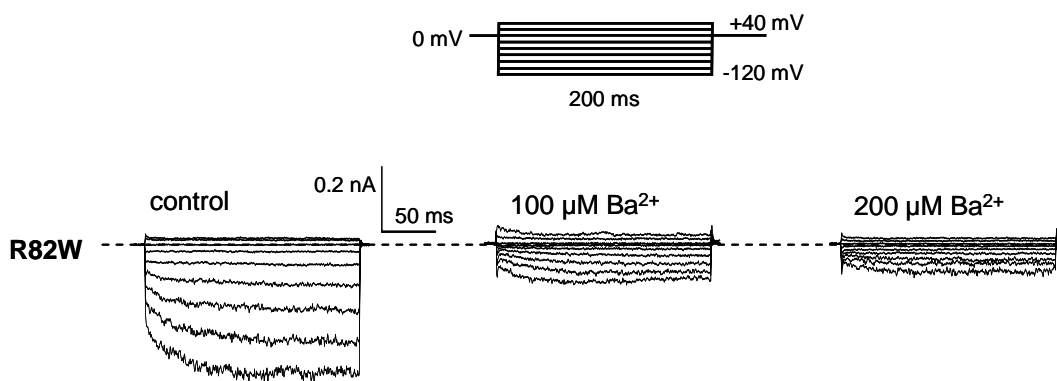


**Fig. 11. Effect of  $[Ba^{2+}]_{out}$  on the steady-state current of R82W mutant Kir2.1 channels.** Inward currents measured in 164.5 mM  $[K^+]_{out}$  under control conditions (*left*) and after addition of 100  $\mu M$  (*middle*) and 200  $\mu M$   $Ba^{2+}$  concentrations (*right*). Cells were held at 0 mV holding potential and currents were elicited as described in legend to Fig. 4.

Inward currents measured through cells transfected with R82W mutant Kir2.1 channels (Fig. 11) were blocked by  $Ba^{2+}$  in a dose-dependent manner. However, the R82W mutant Kir2.1 channels did not show a current decline over time, therefore, I concluded that  $Ba^{2+}$  did not produce a time-dependent block on the R82W mutant Kir2.1 channels (Fig. 11, *middle and left*).

To find out whether  $Ba^{2+}$  can block current through R82W mutant Kir2.1 channels in a voltage-dependent manner, I analyzed and quantified the steady-state currents obtained in the presence and absence of  $Ba^{2+}$  (Fig. 12).

Typical steady-state currents, in 164.5 mM  $K^+$  solution (Fig. 12 A and B control) and  $K^+$  solution with 100 and 500  $\mu M$   $[Ba^{2+}]_{out}$  for WT Kir2.1 (Fig. 12 A) and 100 and 200  $\mu M$   $[Ba^{2+}]_{out}$  for R82W mutant Kir2.1 (Fig. 12 B) at the end of a 200 ms voltage step (shown in Fig. 8, *middle and left*, and in Fig. 11, *middle and left*), were divided by the respective cell capacitance and steady-state current densities were plotted against the applied membrane potential (Fig. 12 A and B). The steady-state current density obtained in the presence of external 100  $\mu M$   $[Ba^{2+}]_{out}$  in WT (Fig. 12 A) and R82W Kir2.1 (Fig. 12 B) was divided by the steady-state current density obtained in the absence of  $Ba^{2+}$  (control) and the ratio was plotted against the membrane potential (Fig. 12 C). The smooth curves represent fits of a Boltzmann equation to the data as described in the legend to Fig. 12.

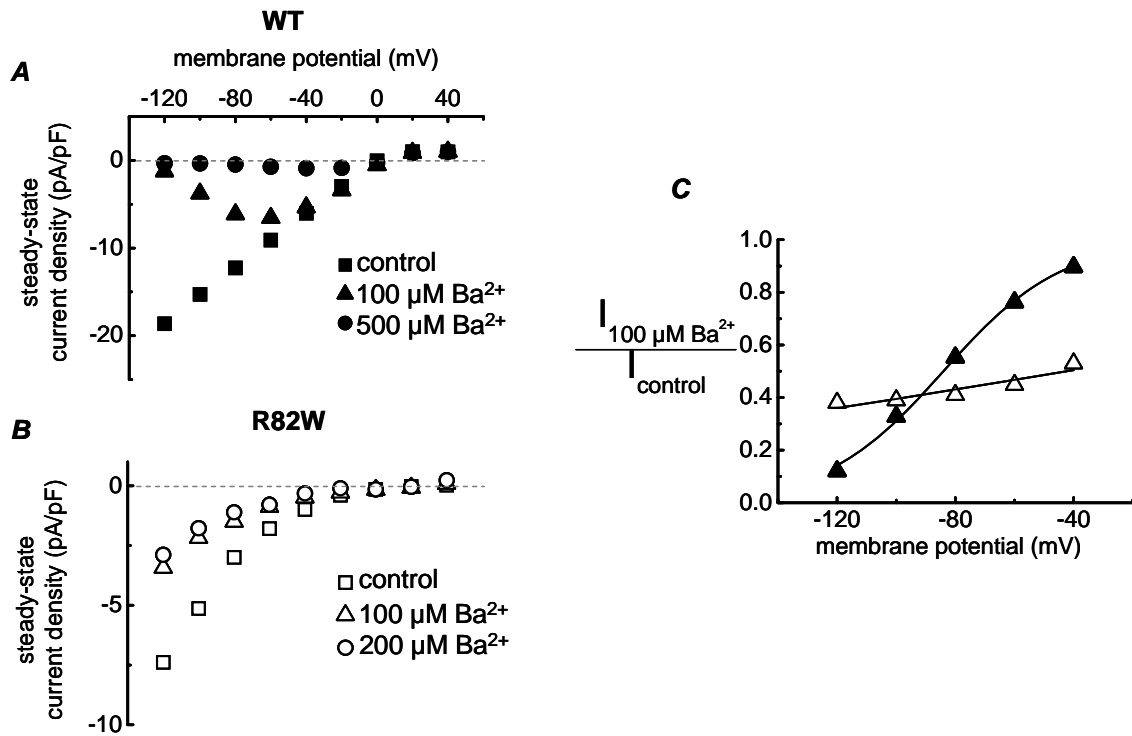


**Fig. 12. Voltage dependence  $[Ba^{2+}]_{out}$  to block steady-state current through WT and R82W mutant Kir2.1 channels.** A, B Steady-state currents from records shown in Fig. 8 and Fig. 10 were divided by the respective cell capacitance and steady-state current density was plotted against the applied membrane potential. C The steady-state current density from A and B obtained in the presence of external  $100 \mu M Ba^{2+}$  (filled triangles for WT and empty triangles for mutant) was divided by the steady-state current density obtained in the absence of  $Ba^{2+}$  (filled squares for WT and empty squares for mutant) and plotted against the membrane potential. The smooth curves represent a Boltzmann equation fitted to the data:

$$I_{100 \mu M Ba^{2+}} / I_{control} = 1 / \{1 + \exp((E_h - E)/k)\},$$

where,  $E_h$  is the voltage at which half the channels are blocked and  $k$  the steepness of the block (mV per e-fold change). The fit parameters for the  $100 \mu M Ba^{2+}$  block were, for the WT Kir2.1 (filled triangles):  $E_h = -84 \pm 1$  mV and  $k = 20 \pm 1$  mV; for the R82W mutant Kir2.1 (empty triangles):  $E_h = -42 \pm 10$  mV and  $k = 135 \pm 30$  mV, respectively. Values are mean from  $n=3$ .

The fit parameters indicated for the WT Kir2.1 that  $Ba^{2+}$  can move more than half-way (60 %) into the electric field from the outside (the partial electrical distance of the  $Ba^{2+}$  binding site across the membrane from the outside,  $\delta = 0.62$ ) and that for R82W mutant Kir2.1 channels  $Ba^{2+}$  can move only about 10 % into the electric field from the outside. The experiments performed with extracellularly applied  $Ba^{2+}$  demonstrated that although the R82 residue is located on the intracellular side of the channel, the R82W mutation leads to structural changes on the outside of the channel.

The R82W mutant Kir2.1 formed functional homomeric channels with small current amplitude, whereas functional homomeric V93I mutant channels resulted in significantly larger inward currents compared to WT Kir2.1 channels. Moreover, R82W mutant subunits were able to form heteromeric channels with WT Kir2.1 channel subunits. I also wanted to investigate the influence of V93I mutant channels on current through WT Kir2.1 channels.

#### ***4.4 Co-transfection experiments with WT and V93I mutant Kir2.1 channels***

To test whether V93I mutant Kir2.1 subunits were able to form functional heteromultimeric channels, I co-transfected COS-7 cells with cDNA coding for WT and for V93I mutant Kir2.1 channels (Fig. 13). Current traces were elicited with the same protocol described for Fig. 4. Current through WT Kir2.1 (Fig. 13 A, *left*) showed strong inward rectification, as already shown and described in Fig. 4. Cells transfected with the V93I mutant Kir2.1 showed significantly larger current amplitudes than those transfected with WT Kir2.1 channels (Fig. 4, column 4 and Fig. 13, *right*). At -120 mV the peak current density was  $-34.7 \pm 2.2$  pA/pF for WT,  $-48.4 \pm 7$  pA/pF for WT+V93I and  $-57.5 \pm 7.7$  pA/pF for V93I mutant.

Co-transfected cells (Fig. 13 A, *middle* and *B* filled circles) showed larger inward currents compared to those recorded in cells transfected with only WT Kir2.1 channels. This indicates the possibility of mutant subunits to co-assemble with WT subunits and form heterotetrameric channels.

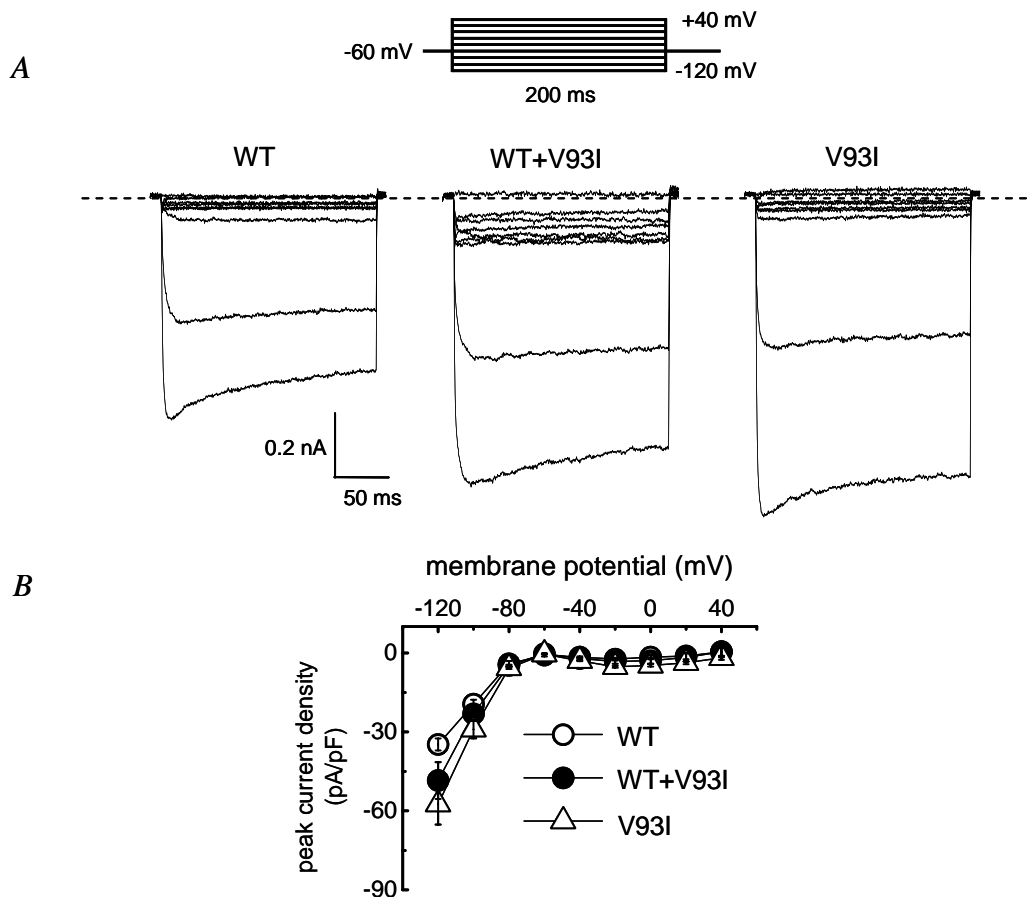


**Fig. 13. Functional consequences of V93I mutation in Kir2.1 channels.** *A* Whole-cell currents measured in COS-7 cells transfected with WT and V93I mutant Kir2.1. Cells were held at -60 mV holding potential and currents were elicited as described in legend to Fig. 4. *B* Peak currents from records shown in *A* and similar experiments were divided by the respective cell capacitance and the peak current density was plotted against the applied membrane potential. Values are mean  $\pm$  S.E.M. ( $n=4-6$ ). S.E.M. is shown as bars when it exceeds the size of the symbol.

Co-transfection of V93I mutant with WT Kir2.1 channels yielded a gain of current compared to WT Kir2.1 channels expressed alone.

The V93I mutation of Kir2.1 substitutes a highly conserved region located in the outer helix of M1 segment in the Kir2.1 channel (Xia *et al.*, 2005). Another highly conserved region among the Kir2 sub-family channels is located in the cytoplasmic C-terminus including amino acid position 215. This position has been described as being part of the PIP<sub>2</sub> binding site in Kir channels. Since PIP<sub>2</sub> regulates Kir channel function, any amino acid substitution occurring here could induce important changes in the biophysical properties of the channel. Therefore I analyzed the G215R mutant Kir2.1 and compared it with other amino acid substitutions at the same position (Hosaka *et al.*, 2003).

#### 4.5 Biophysical characterization of the G215 substitution in WT Kir2.1 channels

In the KCNJ2 gene at the position G215 another amino acid substitution has been previously reported to be associated with ATS, the G215D (Hosaka *et al.*, 2003). Since in my present study both amino acids substitutions (G215R/D) were found in patients with clinical phenotypes associated with Andersen-Tawil syndrome (ATS), I investigated both mutants. To characterize their electrophysiological properties I compared currents in transiently transfected COS-7 cells with cDNA coding for G215R (Fig. 14, *middle*) or G215D (Fig. 14, *right*) mutant Kir2.1 channels. Current traces were elicited with the same protocol described for Fig. 4 and inward currents were compared when cells were transfected with only WT Kir2.1 channels.

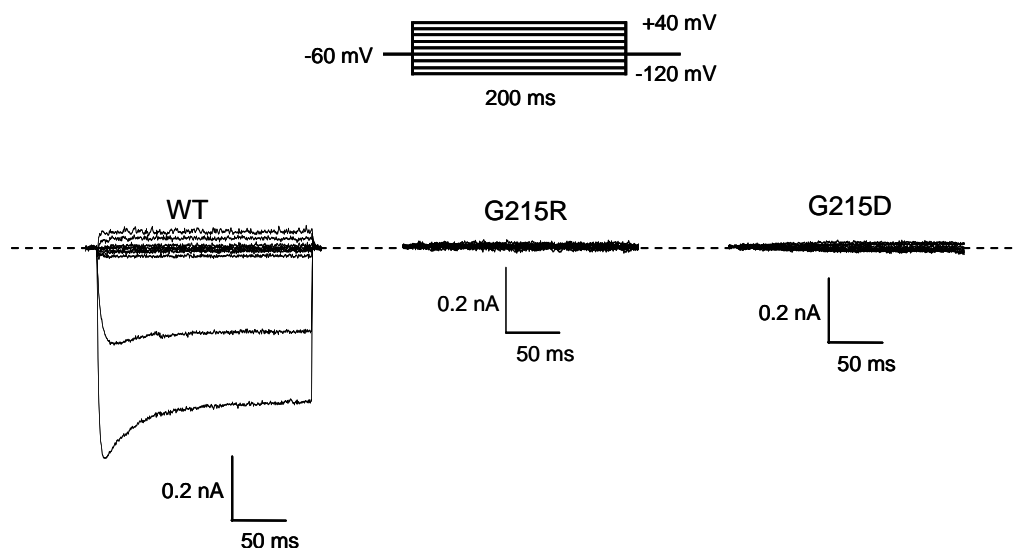


**Fig. 14. Functional consequences of ATS-associated G215 mutations in Kir2.1 channels.** Whole-cell currents measured in COS-7 cells transfected with WT (*left*), G215R (*middle*), and G215D mutant Kir2.1 (*right*). Cells were held at -60 mV holding potential and currents were elicited as described in legend to Fig. 4.

Current through WT Kir2.1 (Fig. 13 A, *left*) showed strong inward rectification, as already shown and described in Fig. 4 and no currents were observed in cells transfected with only G215R or G215D mutant Kir2.1 channels. The lack of current of the G215D mutant Kir2.1 channels confirmed the published data of Hosaka *et al.* (2003), who showed also no current when transfected the G215D in COS-7 cells alone.

Both mutations in Kir2.1 channels at this position, G215R/D, lead to non-functional channels. In the following I wanted to investigate the influence of these mutant channels on the WT Kir2.1 current.

#### 4.5.2 Co-expression of WT with G215D mutant Kir2.1 channels

In whole-cell patch-clamp experiments the G215D mutant Kir2.1 as already shown and described (Fig. 14 A, *right*) resulted in lack of current. Therefore I wanted to see whether co-transfection of this mutant with WT Kir2.1 channels can influence WT channel properties.

To test whether G215D mutant Kir2.1 subunits were able to change the current through WT channels, I co-transfected COS-7 cells with cDNA coding for WT and for G215D mutant Kir2.1 (Fig. 15). Current traces were elicited with the same protocol described for Fig. 4 and inward currents were compared to cells which were transfected with only WT Kir2.1 channels.

Current through WT Kir2.1 (Fig. 15 A, *left*) showed strong inward rectification, as already shown and described in Fig. 4 and no currents were observed in cells transfected with only G215D mutant Kir2.1 channels (Fig. 15 A, *right*). More than half of the WT Kir2.1 current is lost by the co-transfection with G215D mutant Kir2.1 (Fig. 15 A, *middle*).

Several independent co-transfection experiments (WT+ G215D) showed similar results. Peak currents from records shown in Fig. 15 A and similar experiments were divided by the respective cell capacitance and the obtained peak current density was plotted against the applied membrane potential (Fig. 15 B). At -120 mV the peak current density was  $-39.8 \pm 2.4$  pA/pF for WT,  $-10.4 \pm 3$  pA/pF for WT+ G215D and  $-0.33 \pm 0.1$  pA/pF for G215D mutant channels. This loss of current by co-transfection can be best visualized in Fig. 15 B. For electrophysiological experiments, the statistical analysis was performed using one-way ANOVA and Student's unpaired *t*-test with  $P < 0.05$  and  $P < 0.01$ , respectively considered significantly. Inward current densities in the cells co-transfected with WT (0.5  $\mu$ g) plus G215D mutant Kir2.1 (0.5  $\mu$ g) at -120 mV were significantly lower than those in cells transfected with WT Kir2.1 (1  $\mu$ g). The density values of current from 3 independent co-transfection experiments were significantly different ( $P < 0.006$ ) by one-way ANOVA.

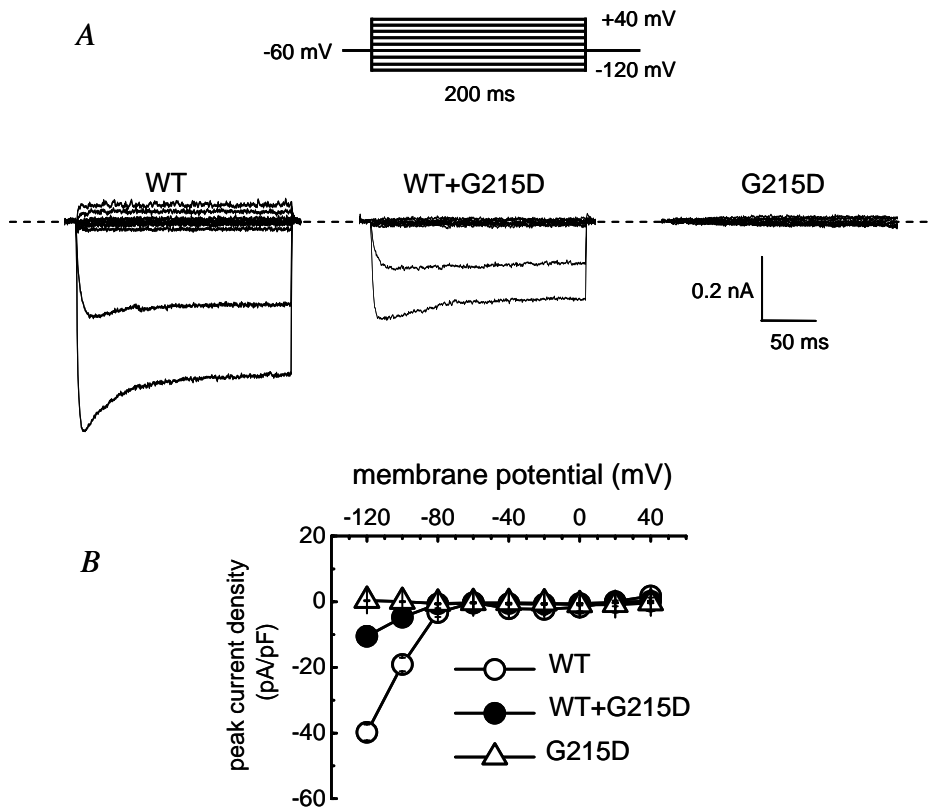


**Fig. 15. Functional characterization of the G215D mutation when co-transfected with the WT Kir2.1 channels.** *A* Whole-cell currents measured in COS-7 cells transfected with WT (*left*), WT+ G215D mutant (*middle*), and G215D mutant alone (*right*). Cells were held at -60 mV holding potential and currents were elicited as described in legend to Fig. 4. *B* Peak currents from records shown in *A* and similar experiments were divided by the respective cell capacitance and the peak current density was plotted against the applied membrane potential. Values are mean  $\pm$  S.E.M. ( $n= 4-6$ ). S.E.M. is shown as bars when it exceeds the size of the symbol.

Co-transfected cells (Fig. 15 *A*, *middle* and *B* filled circles) showed less inward currents compared to those recorded in cells transfected with only WT Kir2.1 channels, indicating the possibility of mutant subunits to co-assemble with WT subunits and form non-functional channels. The co-transfection of WT with G215D mutant Kir2.1 channels confirmed and expanded the observations made by Hosaka *et al.* (2003).

Since G215D mutants showed the possibility to form heterotetrameric channels in combination with WT, it was interesting to investigate the biophysical properties of another mutation occurring at the same position in Kir2.1 channel (G215R). As already shown and described in Fig. 14, both G215 mutations showed loss of channel function.

#### 4.5.3 Co-expression of WT with G215R mutant Kir2.1 channels

The G215R mutant Kir2.1 as already shown and described in Fig. 4 and Fig. 14 lacked inward current when transfected alone (Fig. 14 A, *middle*). Therefore I wanted to see whether co-transfection of this mutant with the WT Kir2.1 changed the expression of WT channels.

To test whether the G215R mutant Kir2.1 subunits were able to form functional heteromultimeric channels, I co-transfected COS-7 cells with cDNA coding for WT and for G215R mutant Kir2.1 channels (Fig. 16). Current traces were elicited with the same protocol described for Fig. 4 and inward currents were compared when cells were transfected with only WT Kir2.1 channels. Current through WT Kir2.1 (Fig. 16 A, *left*) showed strong inward rectification, as already shown and described in Fig. 4 and no currents were observed in cells transfected with only G215R mutant Kir2.1 channels (Fig. 16, A *right*).

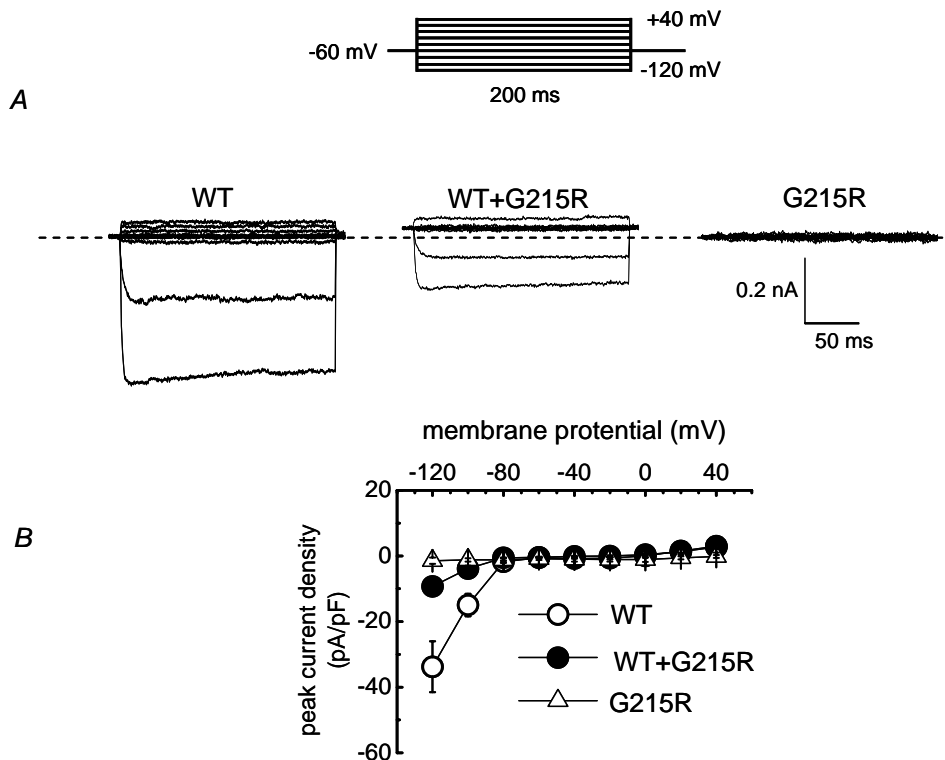


**Fig. 16. Functional characterization of the G215R mutation when co-transfected with WT Kir2.1 channels.** A Whole-cell currents measured in COS-7 cells transfected with WT (*left*), WT plus G215R mutant (*middle*), and G215R mutant alone (*right*). Cells were held at -60 mV holding potential and currents were elicited as described in legend to Fig. 4. B Peak currents from records shown in A and similar experiments were divided by the respective cell capacitance and the peak current density was plotted against the applied membrane potential. Values are mean  $\pm$  S.E.M. (n= 3-6). S.E.M. is shown as bars when it exceeds the size of the symbol.

Heterotetrameric channels of WT + G215R mutant Kir2.1 channels (Fig. 16 A, *middle*) showed an inward current amplitude less than half the size of the current amplitude of the WT Kir2.1 current. At -120 mV the peak current density was  $-33.7 \pm 7.7$  pA/pF for WT,  $-9.2 \pm 1.8$  pA/pF for WT+ G215R and  $-0.4 \pm 0.9$  pA/pF for G215R mutant. This loss of current by co-transfection can be best visualized in Fig. 16 B. For electrophysiological experiments, the statistical analysis was performed using one-way ANOVA and Student's unpaired *t*-test with  $P < 0.05$  and  $P < 0.01$ , respectively considered significantly. Inward current densities in cells co-transfected with WT (0.5  $\mu$ g) plus G215D mutant Kir2.1 (0.5  $\mu$ g) at -120 mV were significantly lower than those in the cells transfected with WT Kir2.1 (1  $\mu$ g). The density values of current from 3 independent co-transfection experiments were significantly different ( $P < 0.002$ ) by one-way ANOVA.

The co-expression of WT with G215R mutant Kir2.1 channels further expanded the observations made by Hosaka *et al.* (2003) concerning the substitution occurring at the same position in the KCNJ2 gene.

Mutations at G215 position lacked inward current when expressed alone and formed non-functional heterotetrameric channels in combination with WT. An alternative explanation for the current loss by the co-transfection could be the mutant might alter the trafficking of the channel to the cell membrane, or alter the channel assembly. To investigate the subcellular distribution of G215R mutant Kir2.1 channels, I performed confocal laser microscopy experiments.

#### **4.5.4 Subcellular localization of WT and G215R mutant Kir2.1 channels**

The functional consequence of most Kir mutations is a disruption of subunit folding and changed trafficking of the channel to the cell surface membrane (Furutani *et al.*, 1999; Delisle *et al.*, 2004; Gong *et al.*, 2005)

G215R mutant Kir2.1 channels showed no current in whole-cell experiments. This situation is consistent with a loss of channel function which could result from alteration of ion permeation through the channel or from the channel's inability to reach the cell surface. To distinguish between these two possibilities, I performed confocal laser microscopy experiments to investigate the subcellular distribution of G215R mutant Kir2.1 channels. Therefore, I transfected COS-7 cells with tagged, fluorescent-labelled WT (WT<sub>i</sub>) and/or with tagged G215R mutant (G215R<sub>i</sub>) Kir2.1 channels, respectively.

Tagging with fluorescent protein did not affect WT Kir2.1 channel function, because a similar current conductance to untagged WT Kir2.1 channels was consistently observed in cells transfected with WT<sub>t</sub> Kir2.1 (Fig. 17, *in black*). Additionally, I observed no current in cells transfected with G215R<sub>t</sub> mutant Kir2.1 channels (Fig. 17, *in red*) which is consistent with the previous experiments where I transfected cells with untagged G215R mutant Kir2.1 channels (Fig. 4 column 5, Fig. 14 *middle*, and Fig. 16 A, *right*).

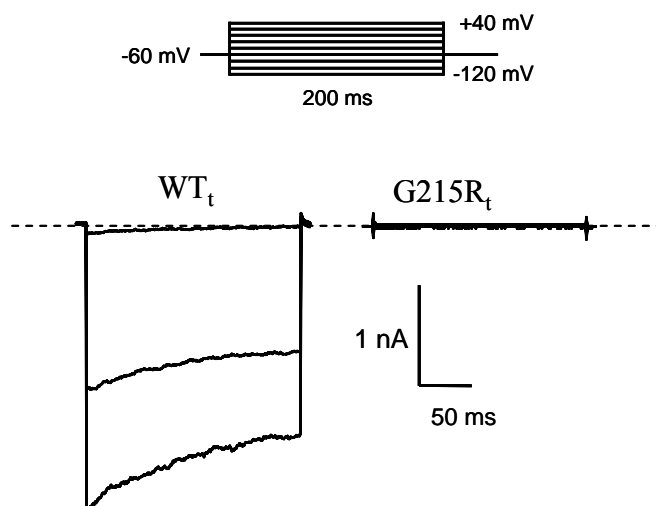


**Fig. 17. Whole-cell currents in COS-7 cells transfected with tagged, fluorescent-labelled WT<sub>t</sub> and tagged G215R<sub>t</sub>.** Cells were held at -60 mV holding potential and currents were elicited as shown and described in legend for Fig. 4. Current traces were corrected for non-specific currents by using the steady-state current at the end of the pulse at -80 mV to subtract from each current trace.

To investigate the subcellular localization of G215R mutant Kir2.1 channels I performed the following confocal laser microscopy experiments:

First, I assessed the subcellular distribution of WT Kir2.1 channels in COS-7 cells, by expressing WT<sub>t</sub> Kir2.1 alone (Fig. 18 *upper left*). In these experiments I observed predominantly staining of the cell membrane.

Second, I transfected G215R<sub>t</sub> mutant Kir2.1 channels alone (Fig. 18 *upper right*) and observed also clear membrane staining.

Third, to see whether co-transfection of WT with G215R mutant Kir2.1 channels influenced the protein localization to the plasma membrane, I co-transfected WT<sub>t</sub> Kir2.1 with the untagged G215R mutant Kir2.1 (Fig. 18 *lower left*) and then, the G215R<sub>t</sub> Kir2.1 with the untagged WT Kir2.1 (Fig. 18 *lower right*).

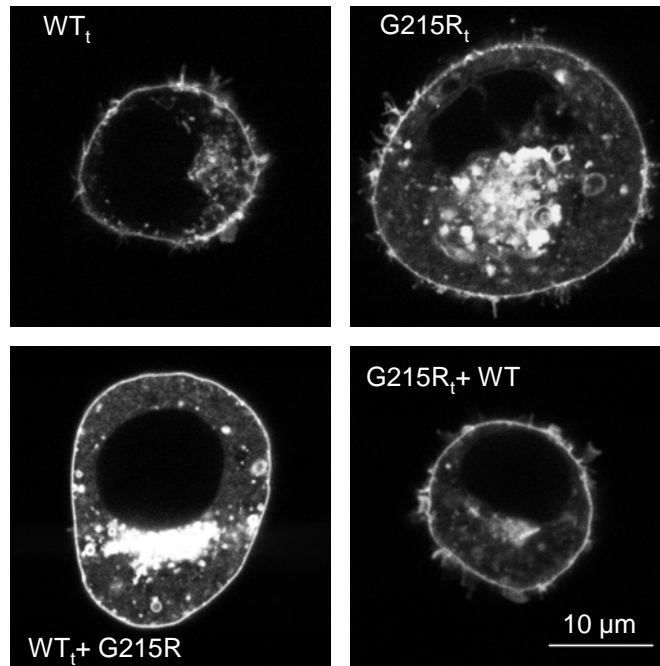


**Fig. 18. Subcellular localization of WT and G215R mutant Kir2.1 channels in COS-7 cells.** Confocal microscopic images of cells transfected with WT<sub>t</sub> Kir2.1 alone (*upper left*), G215R<sub>t</sub> mutant Kir2.1 alone (*upper right*), WT<sub>t</sub> Kir2.1 + untagged G215R mutant Kir2.1 (*lower left*), and G215R<sub>t</sub> mutant Kir2.1 + untagged WT Kir2.1 (*lower right*).

Transfected cells showed a clear membrane localization of WT and G215R channels.

In co-transfection experiments WT and G215R mutant Kir2.1 channels showed a similar plasma membrane staining in comparison to WT or G215R mutant Kir2.1 were transfected alone. In this procedure, 53 of 60 cells transfected with WT<sub>t</sub> Kir2.1 exhibited enhanced fluorescence signals in the plasma membrane and 34 of 50 cells transfected with the G215R<sub>t</sub> mutant Kir2.1 showed a similar fluorescence pattern indicating that the majority of the mutant Kir2.1 channels were expressed in the plasma membrane. A series of fluorescence confocal images revealed that each WT<sub>t</sub> and G215R<sub>t</sub> mutant Kir2.1 channels when co-transfected were distributed similarly in the cell membrane.

The data clearly showed that the G215R mutant Kir2.1 did not induce trafficking problems when transfected alone or in combination with the WT Kir2.1.

As a final overview of the biophysical characterization of the KCNJ2 mutations, I show in Fig. 19 the specific whole-cell conductances of cells transfected with these mutations in combination with the WT.

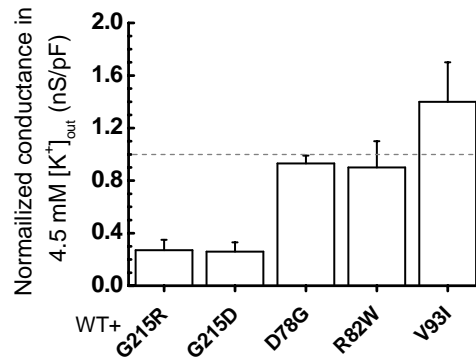


**Fig. 19. Comparison of the co-expression of mutant Kir2.1 in 4.5 mM  $[K^+]_{out}$ .** Each column bar represents the normalized conductance of co-expressed subunits (WT + mutant). Normalization was done by dividing the observed co-expression conductance with the conductance of the WT alone. Values are mean  $\pm$  S.E.M. (n= 2-6).

In order to calculate the percentage of current change in heterotetrameric channels compared to homotetrameric WT channels, the WT expression was considered to be 1. Then each co-transfection was normalized to the respective WT expression.

My results indicate that co-expression of both G215 substitutions with WT channels resulted in current loss of more than 50% compared with the WT channel expression alone. The D78G and R82W mutants formed heterotetrameric channels in combination with the WT channel with similar current amplitude to the homotetrameric WT channel. The V93I mutant resulted in a gain of channel function when expressed alone and formed heterotetrameric channels in combination with the WT with larger current than the homotetrameric WT channels.

My data showed that the decrease (loss of function) or increase (gain of function) in Kir2.1 could account for the heart problems in ATS and AF patients. Additionally, a loss of Kir2.1 channel function will result in instability of the membrane potential in the respective cells thereby leading to depolarization. This will further inactivate sodium channels and reduce or even prevent the generation of action potentials shown to be responsible for hypokalemic periodic paralysis (Jurkat-Rott *et al.*, 2000; Ruff and Cannon, 2000).

In contrary, the gain of function mutations will result in more functional  $K^+$  channels in the respective cells and thereby stabilize the membrane potential. In the clinical characterization of Andersen-Tawil syndrome, patients suffer of arrhythmias and not a single case was reported as presenting with atrial fibrillation. Moreover, Andersen' patients have diverse dysmorphic features whose cause is still unknown. Individuals suffering from

a rare case of atrial fibrillation do not have any characteristic dysmorphic features of ATS and, they have always only short QT interval, which is not characteristic for ATS.

There are still open questions for the implication of the KCNJ2 gene in different heart dysfunctions and for implications of the Kir2.1 channel encoded by this gene, in dysmorphic features of ATS.

## 5 DISCUSSION

The purpose of this study was to characterize electrophysiologically mutations found in the KCNJ2 gene. This gene encodes the Kir2.1 channel and mutations in this gene have been associated with Andersen-Tawil syndrome (ATS) and/or atrial fibrillation (AF) susceptibility. The patients harboured pathogenetic mutations in KCNJ2 gene with four novel mutations (D78G, R82W, V93I and G215R) and one previously reported mutation (G215D).

As an overview of the regions where these mutations are occurring in the Kir2.1 channel I highlighted their localization in the X-ray crystallographic structure of the prokaryotic inward-rectifier K<sup>+</sup> channel KirBac1.1 (Fig. 20).

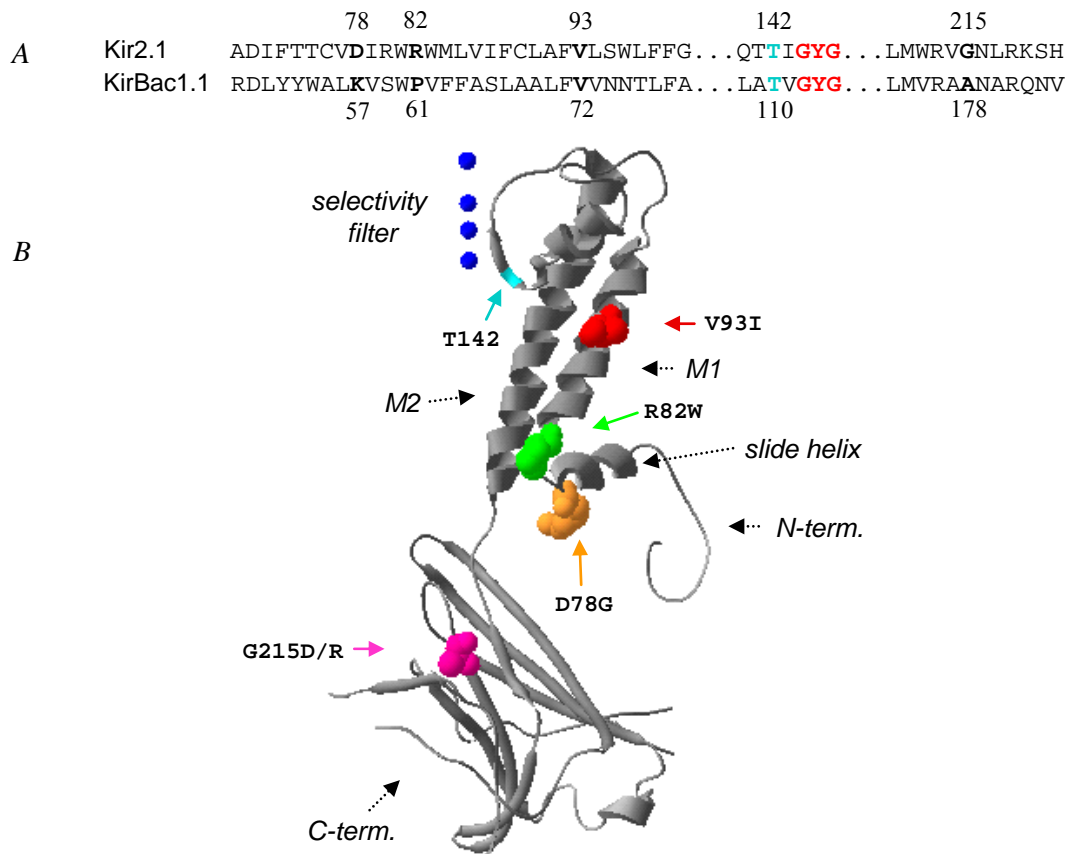


**Fig. 20. Sequence alignment and structure of KirBac1.1.** **A.** Sequence alignment of Kir2.1 and KirBac1.1. Mutations related to ATS and/or AF are in bold; the selectivity filter residues GYG are highlighted in red and the residue T142 involved in the Ba<sup>2+</sup> binding site in cyan. **B.** Homology model of Kir2.1 subunit based on the sequence alignment above. X-ray crystallographic structure (side view) of KirBac1.1 inward-rectifier K<sup>+</sup> channel subunit (PDB number: 1P7B), with residues highlighted in orange (D78G), green (R82W), red (V93I), magenta (G215D/R) and cyan (T142). Represented in blue are K<sup>+</sup> ions in the selectivity filter.

To characterize electrophysiologically the function of these KCNJ2 mutations I performed the whole-cell recording mode of the patch-clamp technique on COS-7 cells. My experiments demonstrated that homomeric channels of the D78G, G215D or G215R mutants did not show any current, whereas the R82W showed little and the V93I mutants did show large currents indicating the formation of functional homomeric channels.

The R82 substitution at the cytoplasmic part of the channel led to structural changes of the outside of the channel, an argument raised by the modified effect of extracellularly applied  $Ba^{2+}$  on R82W mutant channels compared to WT channels. This situation was not expected because the  $Ba^{2+}$  binding site is located extracellularly and far away from the R82 residue.

My data showed that the G215R mutant inhibited the WT channel function by co-assembling with WT subunits, and not by inducing a reduced membrane localization of the channels since the expression of homo- (G215R mutant) and heteromeric (WT + G215R) channels at the membrane were comparable to that of homomeric WT channels.

As a follow-up of this short overview of the above mentioned KCNJ2 mutations I will discuss each of them in more details.

### ***5.1 The D78G mutation***

Transfection of the D78G mutant Kir2.1 resulted in no current. Co-transfection of cDNA coding for the D78G mutant and WT channel resulted in unchanged current-voltage relationships compared to homomeric WT Kir2.1 channels. This strongly suggested that the D78G mutant is able to form heterotetrameric channels with the WT.

The fact that the current is larger in the co-expression compared to the WT current suggests that it must be at least one WT subunit for the D78G mutant channel to be functional. This assemble of mutant subunits with WT subunits allows the formation of functional channels. Alternatively, since the mutant forms functional heteromeric channels and the mutant channel alone is not functional the assembly of mutant subunits with WT subunits could also change the mutant single channel conductance. This supports the idea of normal trafficking to the cell membrane.

My data shows not a clear relevance for all this situations but a simple explanation of what is happening when WT subunits are co-transfected with D78G mutant subunits might be that the mutant channel needs to conjugate with the WT in order to form functional channels.

Recent work published on D78G mutant Kir2.1 channels (Davies *et al.*, 2005) showed similar although not identical results to my data. The authors injected RNA (mutant, WT+ mutant) into *Xenopus* oocytes and measured currents with the two electrode voltage-clamp technique. The co-injection of both RNA resulted in about 50 % less current compared to the single expression of WT RNA. Therefore, the authors concluded that this mutation exhibited a dominant negative effect on WT Kir2.1 channels. I did not observe such an effect in my experiments. An explanation could be that they injected RNA into oocytes whereas, in my experiments I transfected cDNA into a mammalian expression system (COS-7 cells). Additional or different factors could be needed in the cDNA transcription process to the final proteins. Additionally, the correlation between the time needed for the protein expression and the time of analysing the channels' properties could be of important matter.

The D78G mutation occurs in a highly conserved but functionally undetermined region within the N-terminus of the Kir2.1 channel (Davies *et al.*, 2005). Stockklausner *et al.* (2003) reported that the N-terminal region of Kir2.1 is necessary for protein trafficking of this channel from the Golgi complex to the plasma membrane; thus, it could be possible that the D78G mutation affected the sequence required for the export of Kir2.1 from the Golgi complex.

Comparison studies of the crystallographic structure of the prokaryotic Kir channel KirBac1.1 locates this residue within the slide helix (Fig. 19), a channel segment that has been suggested to play a role in the gating process (Lopes *et al.*, 2002). Therefore, I hypothesize that since this D78G mutation is able to form heteromultimeric channels with the WT, it might be that this mutant can only form functional channels in combination/co-assembling with WT channels. It is likely that the gating process in the mutant channel is modified in such a way that no current can be observed in the homotetrameric mutant channel. Only one or two WT subunits per channel might be sufficient to rescue the gating process of the heterotetrameric channel made of mutant and WT subunits.

Another reported property of an N-terminal segment immediately adjacent to M1 (from C54 to V86) revealed through cysteine scanning mutagenesis studies that the majority of amino acids, including the residue D78 are water accessible and probably contribute to the formation of a long and wide intracellular pore vestibule that protrudes into the cytoplasm (Lu *et al.*, 1994). Substitution of the D78 residue might induce another channel conformation in which the intracellular pore vestibule protruding into the cytoplasm is not wider anymore and this might not permit the potassium ions to pass and therefore the

Kir2.1 channel can not conduct current anymore. This might explain a possible situation for single channel conductance alteration by the D78G substitution.

## **5.2 The R82W mutation**

The R82W mutation is located in the N-terminal region of the Kir2.1 channel and could possibly be involved in the formation of a long and wide intracellular pore vestibule that protrudes into the cytoplasm (Lu *et al.*, 1994).

The R82W mutant displayed functional homotetrameric channels with smaller current amplitudes compared to WT channels. It is likely that the gating process in the mutant channel is modified therefore larger current can be observed in the heterotetrameric channels made of mutant and WT subunits. At least one WT subunits per channel might be sufficient to influence the gating process of the heterotetrameric channel. This indicates that the single channel conductance of the R82W mutant channel could be modified by the assembly with WT channel subunits.

### **Effect of Ba<sup>2+</sup> on R82W mutant Kir2.1 channels**

Kir channels show a high sensitivity to external application of Ba<sup>2+</sup> in different cell types. The interaction of divalent cations with Kir channels is thought to occur via two distinct binding sites; a shallow site that barely senses the membrane electric field and, a deeper one located approximately half-way within the membrane electrical field (Alagem *et al.*, 2001). Channel block by Ba<sup>2+</sup> was found to occur through the deeper one (Standen & Stanfield, 1978; Shioya *et al.*, 1993; Reuveny *et al.*, 1996; Sabirov *et al.*, 1997; Shieh *et al.*, 1998). It was described that residue T142 (for location of this position see Fig. 20) which is located in the selectivity filter is involved in the Ba<sup>2+</sup> binding. For all divalent cations, a single ion suffices to block the channel. In most cases of deep site blockers, the block follows first-order kinetics, taking several seconds to reach a steady-state (Standen & Stanfield, 1978; Shieh *et al.*, 1998). An exception is the G-protein-coupled inwardly rectifying potassium channel family, where part of the Ba<sup>2+</sup> block reaches steady state in an immeasurably short time (Carmeliet & Mubagwa, 1986).

Ba<sup>2+</sup> is pushed more than half-way (60 %) into the electric field from the outside by hyperpolarized potentials. In the R82W mutant channels Ba<sup>2+</sup> can move only about 10 % into the electric field from the outside suggesting in this case, that Ba<sup>2+</sup> can not enter the

selectivity filter any more. Therefore I concluded that the R82W mutation affected the Ba<sup>2+</sup> binding site. Since the R82W mutation is located on the intracellular part of the channel, it seems that this amino acid change induced conformational changes at the extracellular side of the channel indicating that mutations in one part of the channel protein induced structural changes in a different part of the protein. Similar observations have been reported for voltage-gated K<sup>+</sup> channels, where mutations in the outer vestibule of the Kv1.3 channel affected the binding side of intracellular verapamil (Rauer and Grissmer, 1996 and 1999) or mutations in the inner vestibule of the Kv1.3 channel affected binding of extracellular tetraethylammonium or kaliotoxin (Dreker and Grissmer, 2005).

### **5.3 The V93I mutation**

The V93I substitution is located in the outer helix of the M1 segment in Kir2.1 channels, which displays a highly conserved sequence among human, domestic guinea pig, pig, dog, cow, Norway rat, rabbit, and house mouse. Due to this highly conserved residue it seems reasonable to assume that the V93I mutation may have important functional consequences (Guo *et al.*, 2002).

My functional analysis on the V93I mutant demonstrated a gain of Kir2.1 channel function. This is in agreement with the results of Xia *et al.* (2005) who reported an increase of the inward-current amplitude when V93I mutant Kir2.1 was transfected alone.

#### **5.3.1 Mechanism of channel function increase by mutations in KCNJ2**

The functional expression of the V93I substitution demonstrated a significant gain of function in inward Kir2.1 current, without affecting kinetics and rectification properties. Co-expression of the V93I mutant with the WT resulted in heteromeric channels which still preserved the gain of channel function mechanism.

A direct effect on channel conductance is more likely, as suggested by the proximity of residue valine 93 to the pore. Only one or two V93I subunits per channel might be sufficient to result in gain of function of the heterotetrameric channel made of mutant and WT subunits.

### **5.3.2 Consequences of channel function increase by mutations in KCNJ2**

Because of the gain of function, the membrane potential of affected cells will be stabilized. Therefore, the atrial cell excitability would be reduced. Gain of function mutations induce earlier repolarization, and shorten the refractory period, making the myocardium susceptible to the development of tachycardia. Thus, the gain of function effect of V93I mutation may create a substrate favourable to a multiple wavelet re-entry, a dominant mechanism of AF. This was proved by observations of WT Kir2.1 overexpression in the mouse heart which led to abnormalities of cardiac excitability and AF (McLerie and Lopatin, 2003). Li *et al* (2004) also reported an overexpression of Kir2.1 in mouse heart to upregulate  $I_{K1}$  and initiate AF. Kir2.1 gain of function mutation is one of the AF molecular bases. My study not only identifies a molecular mechanism of the genetic form of AF, but also sheds light on molecular mechanism of the acquired forms of AF. Kir2.1 channels of  $I_{K1}$  currents may be potential targets for drug therapy of AF.

### **5.4 The G215R/D mutations**

The G215 is a highly conserved amino acid residue among the inward-rectifier  $K^+$  channels. My investigations on mutations occurring at position 215 in the KCNJ2 gene showed that cells transfected with G215D/R mutations alone failed to form functional homomeric channels and more than half of the WT Kir2.1 current density was lost by co-transfection with G215D or G215R mutants Kir2.1. Possible mechanisms for this current reduction will be discussed below.

#### **5.4.1 Mechanism of channel function suppression by mutations associated with ATS**

It has been shown that some mutated subunits co-assemble with WT Kir2.1 subunits and cause a variable degree of dominant negative suppression of channel function (Plaster *et al.*, 2001). This would be consistent with the idea that one or more mutant Kir2.1 subunits within the tetrameric complex would be sufficient to render the channel non-functional.

The reported ATS mutations are distributed throughout different portions of Kir2.1, including the N-terminal intracellular portion, M1 transmembrane, pore, and C-terminal region. Several of these mutations are located in a region implicated in binding membrane associated  $PIP_2$ .

The modification of PIP<sub>2</sub> binding to the mutant Kir2.1 channels may also contribute to the extent of varied dominant negative effects between different mutants. Approximately half of the mutations described in the literature cause channel dysfunction by adversely affecting the binding of PIP<sub>2</sub> (Lopes *et al.*, 2002). PIP<sub>2</sub> is required to stabilize the open state of Kir channels (Huang *et al.*, 1998). It binds directly to Kir channels through interaction between positively charged amino acids of the Kir channel and negatively charged phosphate groups of the lipid.

Three independent sites (residues: 175-206, 207-246 and, 324-365) were located in the C-terminal region of Kir2.1 channels by assaying the binding of overlapping fragments to PIP<sub>2</sub> containing liposomes (Soom *et al.*, 2001).

The G215R/D residues are located within one of the three putative PIP<sub>2</sub> binding sites. Therefore it seems likely that an amino acid substitution at the 215 position can lead to non-functional channels due to alteration of normal PIP<sub>2</sub> channel interaction.

Another ATS mutation (V302M) which also occurs in the C-terminal region could give a possible explanation to the formation of non-functional channels. In the study of Ma *et al.* (2007) a possible mechanism by which V302M alters channel function suggest that this mutation may influence PIP<sub>2</sub> gating indirectly by conformational changes in the G-loop pore and therefore modifying the PIP<sub>2</sub> binding. Similarly, the R82W mutation induced conformational changes in a part of the channel far away from the mutation which then indirectly led to changes in the channel function and pharmacology.

The recently solved Kir2.1 cytoplasmic domain structure (Pegan *et al.*, 2005) gives a possible explanation for the mechanism of change induced conformation. As shown in Fig. 21, the hydrophobic side chain of V302 projects away from the cytoplasmic pore between residues (R218: T309) that are believed to form a salt bridge and hold the G-loop cytoplasmic pore in an open conformation (Pegan *et al.*, 2006).

Based on the apparent position of V302 relative to the salt bridge, Ma *et al.* (2007) hypothesized that channel activity would be sensitive to alterations in the size, shape, and hydrophobicity of side chains at the V302 position. V302 defines the outer boundary of the G-loop and appears to be engaged in Van der Waals interactions with R218. This residue, R218 lies in the PIP<sub>2</sub> binding site and is believed to form a salt bridge with T309.

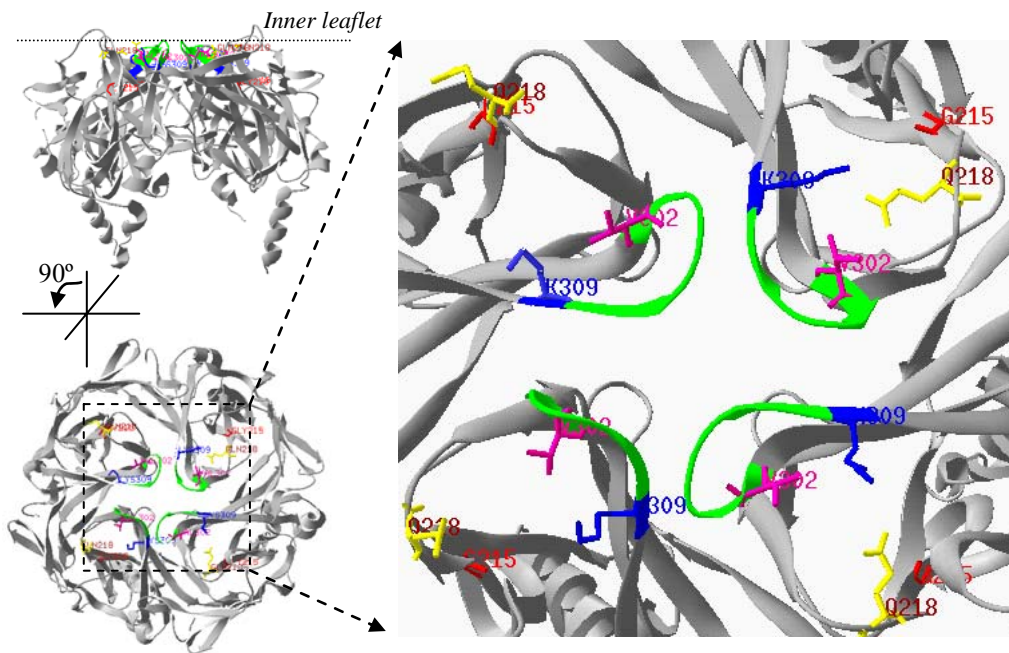


**Fig. 21. Cytoplasmic domains of Kir2.1 as solved by Pegan *et al.* (2005) (PDB number: 1UF).** Highlighted are residues in the G-loop (in green), V302 (magenta), R218 (yellow) and, T309 (blue). G215 (red) might be involved in PIP<sub>2</sub> binding.

The direct interaction between the negative phosphate head group of PIP<sub>2</sub> and several positively charged residues in the N- and C-terminus (e.g. R67, K188, R189, R218, and R312) are essential for activation of Kir2.1 channels (Fan and Makielski, 1997; Shyng *et al.*, 2000; Lopes *et al.*, 2002; Schulze *et al.*, 2003; Zeng *et al.*, 2003). In Fig. 21, I highlighted in red the localization of residue G215 in the proximity of the above mentioned mutations. I suggest that G215 could be involved in the same mechanism and therefore could induce changes in channel gating.

However, the G215D/R mutations could also lead to incorrect assembly or trafficking problems. To assess the cellular localization of G215R Kir2.1 subunits I performed confocal laser scanning microscopy. These experiments showed that G215R mutant channels did not affect the trafficking to the cellular surface. Hosaka *et al.* (2003) investigated the subcellular localization and assembly of the G215D mutant Kir2.1. They performed confocal and FRET experiments. Their results showed similar fluorescence patterns along the plasma membrane and they concluded that the reduction of Kir2.1 channel function (dominant negative effect) is not related to abnormal protein trafficking nor wrong assembly. Therefore, my functional analysis on the G215D mutation was in perfect agreement with Hosaka *et al.* (2003). G215D/R mutants Kir2.1 channels exhibited loss of channel function and a dominant negative effect by tetramultimerization with WT

Kir2.1 channels. In my confocal microscopy study both tagged WT and G215R mutant Kir2.1 channels (pEGFP-N1) were expressed as proteins in the plasma membrane suggesting that the mutant still preserves the ability to localize to the membrane in homo- or heterotrimeric channels with WT subunits.

#### **5.4.2 Consequences of channel function suppression by mutations in KCNJ2**

Dysfunctions due to mutations in the potassium channel gene KCNJ2, which encodes the Kir2.1 subunit, have been related to clinical phenotypes associated with ATS. Recently, KCNJ2 mutations have been identified in affected individuals (Plaster *et al.*, 2001; Ai *et al.*, 2002; Tristani-Firouzi *et al.*, 2002). In ATS, which is an autosomal dominant disorder, affected individuals possess one normal and one mutant KCNJ2 allele.

From the Kir2.1 mutations that have been reported to cause the phenotype of ATS all have been found to result in complete loss of function when expressed alone. Additionally, if these mutants are co-expressed with identical amounts of WT Kir2.1 in order to mimic the heterozygous mutations seen in ATS patients, variable degrees of dominant negative effects were observed. The mechanisms that account for this variability have not been clarified. Previous studies revealed that heterozygous mutations related to ATS may suppress not only the function of the Kir2.1 homotetramer, but also the function of co-expressed Kir2.2 and Kir2.3 heterotetramers (Preisig-Müller *et al.*, 2002).

Additionally, observation on transgenic mice expressing the T75R mutant Kir2.1 (non-functional and with dominant negative suppression on WT) (Lu *et al.*, 2006) in the heart showed prolonged QTc intervals compared to mice expressing the WT Kir2.1. Since the T75R mutated channel affects the polyamine binding this might trigger PIP<sub>2</sub> depletion (Xie *et al.*, 2005) and therefore this might lead to aberrant channel function.

### **5.5 Pathophysiology of clinical features in ATS**

#### **5.5.1 Pathophysiology of the periodic paralysis**

How can a loss of function in the inward rectifier K<sup>+</sup> channel lead to paralysis and to changes of the extracellular K<sup>+</sup> concentration?

Fauler *et al.* (2006) implemented a computer simulation to get insights into the behaviour of muscle by analysis of a simplified system. In their model, both the intra- and extracellular compartments of the model were variable in volume and ion concentrations.

The model consisted of a Na<sup>+</sup>/K<sup>+</sup>-pump, voltage-gated Na<sup>+</sup> and K<sup>+</sup> channels, a chloride and an inwardly rectifying K<sup>+</sup> conductance. In this model, gradual inhibition of the inward-rectifier K<sup>+</sup> conductance depolarized the cell to a critical point at which a further depolarization resulted in a decline of the outward current, thereby destabilizing the resting membrane potential/state. This was followed by a progressive depolarization with almost complete closure of the Kir channel and a concomitant intracellular K<sup>+</sup> accumulation. The system stabilized at a different membrane potential of about -60 mV. This state had the main features of the paralysis in HypoPP i.e. inactivation of voltage-gated Na<sup>+</sup> channels and low [K<sup>+</sup>]<sub>out</sub>.

This model suggested that paralysis in ATS is usually hypokalemic in nature which is in good agreement with previous reports (Davies *et al.*, 2005). According to *in vitro* results on muscle fibers from the G215R patient (Lehmann-Horn, personal communications) RMP measurements gave values of -62 mV in paralysed muscles. This suggested that weakness may be induced by a sustained membrane depolarization which leads to an inactivation of sodium channels and results in loss of membrane excitability until repolarization is regained.

Depolarization decreases the conductance of inward rectifying potassium channels. Hence, in the case of the R82W mutation, thyroid hormone induced depolarization would further decrease the conductance of inward rectifying potassium channels, so that the resting state could be destabilized, promoting a paralyzed state as described above for HypoPP. It looks that in the younger patient the R82W mutation alone does not produce paralysis. However, in combination with other factors, in this case high levels of thyroid hormone, paralytic attacks could be provoked.

In muscle fibres expressing the R82 mutation K<sup>+</sup> outward current might be sufficient to stabilize the RPM under normal conditions but might be insufficient under situation with an increased Na<sup>+</sup> inward current. This hypothesis is confirmed by McArdle and Sansone (1977) who reported an increased Na<sup>+</sup> conductance in muscle fibres under experimental hyperthyroidism leading to a depolarization by about 10 mV.

An open question is why there are some ATS individuals, who do not have a hypokalemic weakness: an individual with G215D from the study reported by Hosaka *et al.* (2003) and the G215D patient of my study are both normo- to hyperkalemic during attacks, similarly, individuals with P186L, R218W, and G300V have hyperkalemic periodic paralysis (Zhang *et al.*, 2005). For these patients, there is no other atypical ATS feature in ECG recordings,

nor a difference in the degree of functional disturbance, nor in the localization or nature of the amino acid substitution. The data of Zhang *et al.* (2005) suggest that the type of dyskalemia is not related to the mutation itself.

### **5.5.2 Pathophysiology of the cardiac arrhythmias**

Loss of function mutations result in less functional K<sup>+</sup> channels and therefore the membrane potential of affected cells will be destabilized and more depolarized compared to cells with a normal K<sup>+</sup> channel expression. In cardiac cells the membrane depolarization and/or membrane potential destabilization might result in cardiac arrhythmias. Similarly, in skeletal muscle this might explain the weakness of contraction or even paralysis observed in patients with ATS.

In the heart, decreased Kir2.1 function may prolong the most terminal phase of repolarization, leading to a lengthening of the QT-time in the ECG (Tristani-Firouzi *et al.*, 2002; Miake *et al.*, 2003). The normal QT-time reflected by ECG is about 300 to 450 ms. If abnormally prolonged or shortened, there is a risk of developing ventricular arrhythmias. An abnormal prolonged QT interval could be due to Long-QT syndrome (LQTS) whereas an abnormal shortened QT interval could be due to Short-QT syndrome. Since the QT-prolongation is only small in ATS, it is probably of minor relevance clinically. The majority of arrhythmias described in ATS seem to arise from the ventricle probably because of higher Kir channel density in ventricular compared to atrial myocytes and their different rectifying properties (Giles *et al.*, 1988; Koumi *et al.*, 1995). In ventricular myocytes, Kir2.1 is preferentially localized to the T-tubular membrane (Clark *et al.*, 2001; Melnyk *et al.*, 2002) where K<sup>+</sup> accumulates during an AP (Pasek *et al.*, 2006).

Arrhythmias in ATS are very different from those seen in Long-QT syndromes especially Torsade-de-Pointe tachycardias are rare in Andersen-patients compared to typical LQTS. The arrhythmia phenotype has many similarities to that seen in Ca<sup>2+</sup>-overloaded states (intracellular myocytes Ca<sup>2+</sup> elevation). Therefore it is reasonable to speculate that a reduction of Kir2.1 current leads to Ca<sup>2+</sup>-overloading. This idea is supported by a recently described mutation, which was associated with catecholaminergic polymorphic ventricular tachycardia (CPVT) (Tester *et al.*, 2006). A reduction in Kir2 prolonged the terminal phase of the cardiac action potential, and led to reduced extracellular K<sup>+</sup>. This situation induced Na<sup>+</sup>/Ca<sup>2+</sup> exchanger-dependent delayed afterdepolarizations and spontaneous arrhythmias (Tristani-Firouzi *et al.*, 2002). These findings suggest that the substrate for arrhythmia

susceptibility in ATS is a distinct from other forms of inherited LQT syndrome. The reduction of Kir2.1 current leading to Ca<sup>2+</sup>-overloading was simulated through a computer model by Tristani-Firouzi *et al.* (2002).

Abnormal sarcoplasmic reticulum calcium cycling is increasingly recognized as an important mechanism for increased ventricular automaticity that leads to lethal ventricular arrhythmia. Previous studies have linked lethal familial arrhythmogenic disorders to mutations in the ryanodine receptor and calsequestrin genes, which interact with junction and triadin to form a macromolecular Ca-signaling complex. The essential physiological effects of junction and its potential regulatory roles in sarcoplasmic reticulum Ca cycling and Ca-dependent cardiac functions, such as myocyte contractility and automaticity, are unknown (Yuan *et al.*, 2007). Studies showed that the process of calcium overloading may play a role as a trigger in the pathogenesis of ventricular arrhythmias (Gilst and Koomen, 1985)

Electrical remodelling in AF is caused by alterations of many different currents, of which I<sub>K1</sub> is only one (McLerie *et al.*, 2003, Li *et al.*, 2004). The clinical data of the family presenting with the V93I mutation Kir2.1 imply that the mutation itself does not produce a complete arrhythmogenic substrate for the development of AF. Therefore I conclude that the V93I mutation does not directly cause AF as has been previously suggested (Roberts 2006). V93I mutation may play a role in initiating and/or maintaining AF by increasing the Kir channel conductance.

## 6 SUMMARY

In this study I characterized electrophysiologically mutations found in the KCNJ2 gene associated with Andersen-Tawil syndrome (ATS) and atrial tachycardia (AT).

- 1) My findings suggest that the **D78G** mutation resulted in a complete loss of function when expressed alone. The co-transfection of this mutation with WT restored the current, indicating the possibility of mutant subunits to co-assemble with WT subunits and form functional heterotetrameric channels. This gives evidence for an autosomal recessive inheritance.
- 2) **R82W** mutant Kir2.1 channels had smaller inward currents compared to WT. A different time course of inward current activation was observed compared to WT channels. If this mutation was co-expressed with identical amounts of WT in order to mimic the heterozygous situation seen in ATS patients, the mutation restored the current. The time constant of Ba<sup>2+</sup> block for the WT channels showed an exponential voltage-dependency (e-fold: 34±1 mV of depolarization), suggesting that one Ba<sup>2+</sup> moves about more than half-way into the membrane electrical field. These observations are in agreement with published data of Alagem *et al.* (2001). In the R82W mutant channel, Ba<sup>2+</sup> can move only about 10% into the electric field from the outside of the channel. It seems that replacing the arginine at position 82 with tryptophan induced conformational changes in the extracellular side of the channel thereby affecting the Ba<sup>2+</sup> binding site.
- 3) **G215D/R** mutant Kir2.1 channels failed to form functional homomeric channels. The WT current density was reduced by more than 50 % by co-expression experiments, indicating the impossibility of mutant subunits to form functional heterotetrameric channels. In mammalian cells the mutant localized to the membrane and showed similar fluorescence patterns along the plasma membrane. Therefore the dominant reduction of Kir2.1 channel function can not be due to abnormal protein trafficking.
- 4) Current through the **V93I** mutant Kir2.1 channels was larger in comparison to WT. This is in agreement with the results of Xia *et al.* (2005) who reported an increase of the inward-current amplitude in homomeric V93I channels. Additionally, co-transfection of V93I mutants with WT yielded a gain of current compared to homomeric WT channels. The clinical data of the patient with the V93I mutation imply that the mutation itself does not produce a complete arrhythmogenic

substrate for the development of atrial fibrillation (AF). Therefore I conclude that the V93I mutation does not directly cause AF as has been previously suggested. The V93I mutation may favour AF by reducing the effective refractory period and the conduction velocity.

My results support the studies on ATS and AF susceptibility causing mutations and extend the findings on already published KCNJ2 mutations: D71V, R218W, (Plaster *et al.*, 2001), D78G (Davies *et al.*, 2005), T192A (Ai *et al.*, 2002), V93I (Xia *et al.*, 2005) and G215D Kir2.1 (Hosaka *et al.*, 2003).

Possible implications for ATS could be linked to a loss of Kir2.1 channel function. This will result in instability of membrane potential in the respective cells thereby leading to depolarization. This will further inactivate the sodium channels and reduce or even prevent the generation of APs shown to be responsible for hypokalemic periodic paralysis (Jurkat-Rott *et al.*, 2000; Ruff and Cannon, 2000).

In contrary, the gain of function mutations will result in more functional K<sup>+</sup> channels in the respective cells and thereby a more stable membrane potential. In cardiac cells this could lead to problems in the generation of APs therefore resulting in abnormalities of cardiac excitability and AF (McLerie *et al.*, 2003; Xia *et al.*, 2005). In atrial cells the effective refractory period and the velocity at impulse propagation are reduced. Both contribute to maintain atrial fibrillation.

Successful treatment of ATS requires separate therapeutic interventions to treat cardiac and skeletal muscle symptoms. Current treatment modalities are based on known effective treatments for periodic paralysis.

## 7 REFERENCE

- Ai, T., Y. Fujiwara, K. Tsuji, H. Otani, S. Nakano, Y. Kubo and M. Horie (2002) Novel KCNJ2 mutation in familial periodic paralysis with ventricular dysrhythmia *Circulation* **105** (22): 2592-4.
- Alagem, N., M. Dvir and E. Reuveny (2001) Mechanism of Ba(2+) block of a mouse inwardly rectifying K<sup>+</sup> channel: differential contribution by two discrete residues *J Physiol* **534** (Pt. 2): 381-93.
- Andelfinger, G., A. R. Tapper, R. C. Welch, C. G. Vanoye, A. L. George, Jr. and D. W. Benson (2002) KCNJ2 mutation results in Andersen syndrome with sex-specific cardiac and skeletal muscle phenotypes *Am J Hum Genet* **71** (3): 663-8.
- Andersen, E. D., P. A. Krasilnikoff and H. Overvad (1971) Intermittent muscular weakness, extrasystoles, and multiple developmental anomalies. A new syndrome? *Acta Paediatr Scand* **60** (5): 559-64.
- Babila, T., A. Moscucci, H. Wang, F. E. Weaver and G. Koren (1994) Assembly of mammalian voltage-gated potassium channels: evidence for an important role of the first transmembrane segment *Neuron* **12** (3): 615-26.
- Bendahhou, S., M. R. Donaldson, N. M. Plaster, M. Tristani-Firouzi, Y. H. Fu and L. J. Ptacek (2003) Defective potassium channel Kir2.1 trafficking underlies Andersen-Tawil syndrome *J Biol Chem* **278** (51): 51779-85.
- Bendahhou, S., E. Fournier, D. Sternberg, G. Bassez, A. Furby, C. Sereni, M. R. Donaldson, M. M. Larroque, B. Fontaine and J. Barhanin (2005) In vivo and in vitro functional characterization of Andersen's syndrome mutations *J Physiol* **565** (Pt 3): 731-41.
- Biggin, P. C., T. Roosild and S. Choe (2000) Potassium channel structure: domain by domain *Curr Opin Struct Biol* **10** (4): 456-61.
- Butt, A. M. and A. Kalsi (2006) Inwardly rectifying potassium channels (Kir) in central nervous system glia: a special role for Kir4.1 in glial functions *J Cell Mol Med* **10** (1): 33-44.
- Chen, L., D. Segal, N. A. Hukriede, A. V. Podtelejnikov, D. Bayarsaihan, J. A. Kennison, V. V. Ogryzko, I. B. Dawid and H. Westphal (2002) Ssdp proteins interact with the LIM-domain-binding protein Ldb1 to regulate development *Proc Natl Acad Sci U S A* **99** (22): 14320-5.

- Cnd L. G. Palmer (1998) Permeation and gating of an inwardly rectifying potassium channel, H. Sackin aum channel. Evidence for a variable energy well *J Gen Physiol* **112** (4): 433-46.
- Chuang, H., Y. N. Jan and L. Y. Jan (1997) Regulation of IRK3 inward rectifier K<sup>+</sup> channel by m1 acetylcholine receptor and intracellular magnesium *Cell* **89** (7): 1121-32.
- Clark, R. B., A. Tremblay, P. Melnyk, B. G. Allen, W. R. Giles and C. Fiset (2001) T-tubule localization of the inward-rectifier K(+) channel in mouse ventricular myocytes: a role in K(+) accumulation *J Physiol* **537** (Pt 3): 979-92.
- Cortes, D. M., L. G. Cuello and E. Perozo (2001) Molecular architecture of full-length KcsA: role of cytoplasmic domains in ion permeation and activation gating *J Gen Physiol* **117** (2): 165-80.
- Davies, N. P., P. Imbrici, D. Fialho, C. Herd, L. G. Bilsland, A. Weber, R. Mueller, D. Hilton-Jones, J. Ealing, B. R. Boothman, P. Giunti, L. M. Parsons, M. Thomas, A. Y. Manzur, K. Jurkat-Rott, F. Lehmann-Horn, P. F. Chinnery, M. Rose, D. M. Kullmann and M. G. Hanna (2005) Andersen-Tawil syndrome: new potassium channel mutations and possible phenotypic variation *Neurology* **65** (7): 1083-9.
- Deal, K. K., S. K. England and M. M. Tamkun (1996) Molecular physiology of cardiac potassium channels *Physiol Rev* **76** (1): 49-67.
- Derst, C., M. Konrad, A. Kockerling, L. Karolyi, G. Deschenes, J. Daut, A. Karschin and H. W. Seyberth (1997) Mutations in the ROMK gene in antenatal Bartter syndrome are associated with impaired K<sup>+</sup> channel function *Biochem Biophys Res Commun* **230** (3): 641-5.
- Dhamoon, A. S., S. V. Pandit, F. Sarmast, K. R. Parisian, P. Guha, Y. Li, S. Bagwe, S. M. Taffet and J. M. Anumonwo (2004) Unique Kir2.x properties determine regional and species differences in the cardiac inward rectifier K<sup>+</sup> current *Circ Res* **94** (10): 1332-9.
- Donaldson, M. R., J. L. Jensen, M. Tristani-Firouzi, R. Tawil, S. Bendahhou, W. A. Suarez, A. M. Cobo, J. J. Poza, E. Behr, J. Wagstaff, P. Szepetowski, S. Pereira, T. Mozaffar, D. M. Escolar, Y. H. Fu and L. J. Ptacek (2003) PIP2 binding residues of Kir2.1 are common targets of mutations causing Andersen syndrome *Neurology* **60** (11): 1811-6.

- Donaldson, M. R., G. Yoon, Y. H. Fu and L. J. Ptacek (2004) Andersen-Tawil syndrome: a model of clinical variability, pleiotropy, and genetic heterogeneity *Ann Med* **36 Suppl 1**: 92-7.
- Doupnik, C. A., N. Davidson and H. A. Lester (1995) The inward rectifier potassium channel family *Curr Opin Neurobiol* **5** (3): 268-77.
- Doyle, D. A., J. Morais Cabral, R. A. Pfuetzner, A. Kuo, J. M. Gulbis, S. L. Cohen, B. T. Chait and R. MacKinnon (1998) The structure of the potassium channel: molecular basis of K<sup>+</sup> conduction and selectivity *Science* **280** (5360): 69-77.
- Dreker, T. and S. Grissmer (2005) Investigation of the phenylalkylamine binding site in hKv1.3 (H399T), a mutant with a reduced C-type inactivated state *Mol Pharmacol* **68** (4): 966-73.
- Du, X., H. Zhang, C. Lopes, T. Mirshahi, T. Rohacs and D. E. Logothetis (2004) Characteristic interactions with phosphatidylinositol 4,5-bisphosphate determine regulation of kir channels by diverse modulators *J Biol Chem* **279** (36): 37271-81.
- Durell, S. R., H. R. Guy, N. Arispe, E. Rojas and H. B. Pollard (1994) Theoretical models of the ion channel structure of amyloid beta-protein *Biophys J* **67** (6): 2137-45.
- Fakler, B., C. T. Bond, J. P. Adelman and J. P. Ruppersberg (1996) Heterooligomeric assembly of inward-rectifier K<sup>+</sup> channels from subunits of different subfamilies: Kir2.1 (IRK1) and Kir4.1 (BIR10) *Pflugers Arch* **433** (1-2): 77-83.
- Fanger, C. M., S. Ghanshani, N. J. Logsdon, H. Rauer, K. Kalman, J. Zhou, K. Beckingham, K. G. Chandy, M. D. Cahalan and J. Aiyar (1999) Calmodulin mediates calcium-dependent activation of the intermediate conductance KCa channel, IKCa1 *J Biol Chem* **274** (9): 5746-54.
- Fauler, M. Jurkat-Rott K. and Lehmann-Horn F.(2007) the dyskalemic periodic paralysis of Andersen-Tawil syndrome-Unravelled by computer simulation? *Biophys. J*
- Feliciello, I. and G. Chinali (1993) A modified alkaline lysis method for the preparation of highly purified plasmid DNA from Escherichia coli *Anal Biochem* **212** (2): 394-401.
- Ficker, E., M. Tagliatela, B. A. Wible, C. M. Henley and A. M. Brown (1994) Spermine and spermidine as gating molecules for inward rectifier K<sup>+</sup> channels *Science* **266** (5187): 1068-72.
- Finley, M., C. Arrabit, C. Fowler, K. F. Suen and P. A. Slesinger (2004) betaL-betaM loop in the C-terminal domain of G protein-activated inwardly rectifying K(+) channels is important for G(beta gamma) subunit activation *J Physiol* **555** (Pt 3): 643-57.

- Glowatzki, E., G. Fakler, U. Brandle, U. Rexhausen, H. P. Zenner, J. P. Ruppersberg and B. Fakler (1995) Subunit-dependent assembly of inward-rectifier K<sup>+</sup> channels *Proc Biol Sci* **261** (1361): 251-61.
- Grafe, P., S. Quasthoff, M. Strupp and F. Lehmann-Horn (1990) Enhancement of K<sup>+</sup> conductance improves in vitro the contraction force of skeletal muscle in hypokalemic periodic paralysis *Muscle Nerve* **13** (5): 451-7.
- Guo, D. and Z. Lu (2003) Interaction mechanisms between polyamines and IRK1 inward rectifier K<sup>+</sup> channels *J Gen Physiol* **122** (5): 485-500.
- Hamill, O. P., A. Marty, E. Neher, B. Sakmann and F. J. Sigworth (1981) Improved patch-clamp techniques for high-resolution current recording from cells and cell-free membrane patches *Pflugers Arch* **391** (2): 85-100.
- Harrison, A. P. and T. Clausen (1998) Thyroid hormone-induced upregulation of Na<sup>+</sup> channels and Na(+)-K<sup>+</sup> pumps: implications for contractility *Am J Physiol* **274** (3 Pt 2): R864-7.
- Hille, B. (1992) G protein-coupled mechanisms and nervous signaling *Neuron* **9** (2): 187-95.
- Hodgkin, A. L., A. F. Huxley and B. Katz (1952) Measurement of current-voltage relations in the membrane of the giant axon of *Loligo* *J Physiol* **116** (4): 424-48.
- Hosaka, Y., H. Hanawa, T. Washizuka, M. Chinushi, F. Yamashita, T. Yoshida, S. Komura, H. Watanabe and Y. Aizawa (2003) Function, subcellular localization and assembly of a novel mutation of KCNJ2 in Andersen's syndrome *J Mol Cell Cardiol* **35** (4): 409-15.
- Inagaki, N., T. Gono, J. P. t. Clement, N. Namba, J. Inazawa, G. Gonzalez, L. Aguilar-Bryan, S. Seino and J. Bryan (1995) Reconstitution of IKATP: an inward rectifier subunit plus the sulfonylurea receptor *Science* **270** (5239): 1166-70.
- Isomoto, S., C. Kondo and Y. Kurachi (1997) Inwardly rectifying potassium channels: their molecular heterogeneity and function *Jpn J Physiol* **47** (1): 11-39.
- Isomoto, S. and Y. Kurachi (1997) Function, regulation, pharmacology, and molecular structure of ATP-sensitive K<sup>+</sup> channels in the cardiovascular system *J Cardiovasc Electrophysiol* **8** (12): 1431-46.
- Isomoto, S., M. Yamada, Y. Horio and Y. Kurachi (1997) Molecular aspects of ATP-sensitive K<sup>+</sup> channels in the cardiovascular system *Jpn J Physiol* **47 Suppl 1**: S5-6.
- Jiang, Y., A. Lee, J. Chen, V. Ruta, M. Cadene, B. T. Chait and R. MacKinnon (2003 a) X-ray structure of a voltage-dependent K<sup>+</sup> channel *Nature* **423** (6935): 33-41.

- Jiang, Y., V. Ruta, J. Chen, A. Lee and R. MacKinnon (2003 b) The principle of gating charge movement in a voltage-dependent K<sup>+</sup> channel *Nature* **423** (6935): 42-8.
- Jurkat-Rott, K. and F. Lehmann-Horn (2005) Muscle channelopathies and critical points in functional and genetic studies *J Clin Invest* **115** (8): 2000-9.
- Jurkat-Rott, K., F. Lehmann-Horn, A. Elbaz, R. Heine, R. G. Gregg, K. Hogan, P. A. Powers, P. Lapie, J. E. Vale-Santos, J. Weissenbach and et al. (1994) A calcium channel mutation causing hypokalemic periodic paralysis *Hum Mol Genet* **3** (8): 1415-9.
- Jurkat-Rott, K., N. Mitrovic, C. Hang, A. Kouzmekine, P. Iaizzo, J. Herzog, H. Lerche, S. Nicole, J. Vale-Santos, D. Chauveau, B. Fontaine and F. Lehmann-Horn (2000) Voltage-sensor sodium channel mutations cause hypokalemic periodic paralysis type 2 by enhanced inactivation and reduced current *Proc Natl Acad Sci U S A* **97** (17): 9549-54.
- Karkanis, T., S. Li, J. G. Pickering and S. M. Sims (2003) Plasticity of KIR channels in human smooth muscle cells from internal thoracic artery *Am J Physiol Heart Circ Physiol* **284** (6): H2325-34.
- Katz, B. (1949) The efferent regulation of the muscle spindle in the frog *J Exp Biol* **26** (2): 201-17.
- Katz, B. (1949) Meniere's syndrome; a practical outline of treatments *Ann West Med Surg* **3** (10): 360-2.
- Krapivinsky, G., E. A. Gordon, K. Wickman, B. Velimirovic, L. Krapivinsky and D. E. Clapham (1995) The G-protein-gated atrial K<sup>+</sup> channel IKACH is a heteromultimer of two inwardly rectifying K<sup>(+)</sup>-channel proteins *Nature* **374** (6518): 135-41.
- Kubo, Y. and Y. Murata (2001) Control of rectification and permeation by two distinct sites after the second transmembrane region in Kir2.1 K<sup>+</sup> channel *J Physiol* **531** (Pt 3): 645-60.
- Kubo, Y., E. Reuveny, P. A. Slesinger, Y. N. Jan and L. Y. Jan (1993) Primary structure and functional expression of a rat G-protein-coupled muscarinic potassium channel *Nature* **364** (6440): 802-6.
- Kuo, A., J. M. Gulbis, J. F. Antcliff, T. Rahman, E. D. Lowe, J. Zimmer, J. Cuthbertson, F. M. Ashcroft, T. Ezaki and D. A. Doyle (2003) Crystal structure of the potassium channel KirBac1.1 in the closed state *Science* **300** (5627): 1922-6.
- Lehmann-Horn, F. and P. A. Iaizzo (1990) Resealed fiber segments for the study of the pathophysiology of human skeletal muscle *Muscle Nerve* **13** (3): 222-31.

- Leonoudakis, D., L. R. Conti, C. M. Radeke, L. M. McGuire and C. A. Vandenberg (2004) A multiprotein trafficking complex composed of SAP97, CASK, Veli, and Mint1 is associated with inward rectifier Kir2 potassium channels *J Biol Chem* **279** (18): 19051-63.
- Li, J., M. McLerie and A. N. Lopatin (2004) Transgenic upregulation of IK1 in the mouse heart leads to multiple abnormalities of cardiac excitability *Am J Physiol Heart Circ Physiol* **287** (6): H2790-802.
- Lopatin, A. N., E. N. Makhina and C. G. Nichols (1994) Potassium channel block by cytoplasmic polyamines as the mechanism of intrinsic rectification *Nature* **372** (6504): 366-9.
- Lopatin, A. N. and C. G. Nichols (1996) [K<sup>+</sup>] dependence of polyamine-induced rectification in inward rectifier potassium channels (IRK1, Kir2.1) *J Gen Physiol* **108** (2): 105-13.
- Lopes, C. M., H. Zhang, T. Rohacs, T. Jin, J. Yang and D. E. Logothetis (2002) Alterations in conserved Kir channel-PIP2 interactions underlie channelopathies *Neuron* **34** (6): 933-44.
- Loussouarn, G., E. N. Makhina, T. Rose and C. G. Nichols (2000) Structure and dynamics of the pore of inwardly rectifying K(ATP) channels *J Biol Chem* **275** (2): 1137-44.
- Lu, Z. and R. MacKinnon (1994) Electrostatic tuning of Mg<sup>2+</sup> affinity in an inward-rectifier K<sup>+</sup> channel *Nature* **371** (6494): 243-6.
- Ma, D., X. D. Tang, T. B. Rogers and P. A. Welling (2007) An andersen-Tawil syndrome mutation in Kir2.1 (V302M) alters the G-loop cytoplasmic K<sup>+</sup> conduction pathway *J Biol Chem* **282** (8): 5781-9.
- MacKinnon, R. (1991) Determination of the subunit stoichiometry of a voltage-activated potassium channel *Nature* **350** (6315): 232-5.
- Mandel, M. and A. Higa (1970) Calcium-dependent bacteriophage DNA infection *J Mol Biol* **53** (1): 159-62.
- McArdle, J. J. and F. M. Sansone (1977) Re-innervation of fast and slow twitch muscle following nerve crush at birth *J Physiol* **271** (3): 567-86.
- McLerie, M. and A. N. Lopatin (2003) Dominant-negative suppression of I(K1) in the mouse heart leads to altered cardiac excitability *J Mol Cell Cardiol* **35** (4): 367-78.
- Melnyk, P., L. Zhang, A. Shrier and S. Nattel (2002) Differential distribution of Kir2.1 and Kir2.3 subunits in canine atrium and ventricle *Am J Physiol Heart Circ Physiol* **283** (3): H1123-33.

- Miake, J., E. Marban and H. B. Nuss (2003) Functional role of inward rectifier current in heart probed by Kir2.1 overexpression and dominant-negative suppression *J Clin Invest* **111** (10): 1529-36.
- Minor, D. L., Jr., S. J. Masseling, Y. N. Jan and L. Y. Jan (1999) Transmembrane structure of an inwardly rectifying potassium channel *Cell* **96** (6): 879-91.
- Neusch, C., J. H. Weishaupt and M. Bahr (2003) Kir channels in the CNS: emerging new roles and implications for neurological diseases *Cell Tissue Res* **311** (2): 131-8.
- Nicoll, R. A., R. C. Malenka and J. A. Kauer (1990) Functional comparison of neurotransmitter receptor subtypes in mammalian central nervous system *Physiol Rev* **70** (2): 513-65.
- Papazian, D. M., L. C. Timpe, Y. N. Jan and L. Y. Jan (1991) Alteration of voltage-dependence of Shaker potassium channel by mutations in the S4 sequence *Nature* **349** (6307): 305-10.
- Pasek, M., J. Simurda and G. Christie (2006) The functional role of cardiac T-tubules explored in a model of rat ventricular myocytes *Philos Transact A Math Phys Eng Sci* **364** (1842): 1187-206.
- Pegan, S., C. Arrabit, P. A. Slesinger and S. Choe (2006) Andersen's syndrome mutation effects on the structure and assembly of the cytoplasmic domains of Kir2.1 *Biochemistry* **45** (28): 8599-606.
- Pegan, S., C. Arrabit, W. Zhou, W. Kwiatkowski, A. Collins, P. A. Slesinger and S. Choe (2005) Cytoplasmic domain structures of Kir2.1 and Kir3.1 show sites for modulating gating and rectification *Nat Neurosci* **8** (3): 279-87.
- Perier, F., C. M. Radeke and C. A. Vandenberg (1994) Primary structure and characterization of a small-conductance inwardly rectifying potassium channel from human hippocampus *Proc Natl Acad Sci U S A* **91** (13): 6240-4.
- Plaster, N. M., R. Tawil, M. Tristani-Firouzi, S. Canun, S. Bendahhou, A. Tsunoda, M. R. Donaldson, S. T. Iannaccone, E. Brunt, R. Barohn, J. Clark, F. Deymeer, A. L. George, Jr., F. A. Fish, A. Hahn, A. Nitu, C. Ozdemir, P. Serdaroglu, S. H. Subramony, G. Wolfe, Y. H. Fu and L. J. Ptacek (2001) Mutations in Kir2.1 cause the developmental and episodic electrical phenotypes of Andersen's syndrome *Cell* **105** (4): 511-9.
- Perozo, E., D. M. Cortes and L. G. Cuello (1999) Structural rearrangements underlying K<sup>+</sup>-channel activation gating *Science* **285** (5424): 73-8.

- Premkumar, L. S. and P. W. Gage (1994) Potassium channels activated by GABAB agonists and serotonin in cultured hippocampal neurons *J Neurophysiol* **71** (6): 2570-5.
- Priori, S. G., S. V. Pandit, I. Rivolta, O. Berenfeld, E. Ronchetti, A. Dhamoon, C. Napolitano, J. Anumonwo, M. R. di Barletta, S. Gudapakkam, G. Bosi, M. Stramba-Badiale and J. Jalife (2005) A novel form of short QT syndrome (SQT3) is caused by a mutation in the KCNJ2 gene *Circ Res* **96** (7): 800-7.
- Proks, P., J. F. Antcliff and F. M. Ashcroft (2003) The ligand-sensitive gate of a potassium channel lies close to the selectivity filter *EMBO Rep* **4** (1): 70-5.
- Raab-Graham, K. F. and C. A. Vandenberg (1998) Tetrameric subunit structure of the native brain inwardly rectifying potassium channel Kir 2.2 *J Biol Chem* **273** (31): 19699-707.
- Rauer, H. and S. Grissmer (1996) Evidence for an internal phenylalkylamine action on the voltage-gated potassium channel Kv1.3 *Mol Pharmacol* **50** (6): 1625-34.
- Rauer, H. and S. Grissmer (1999) The effect of deep pore mutations on the action of phenylalkylamines on the Kv1.3 potassium channel *Br J Pharmacol* **127** (5): 1065-74.
- Reimann, F. and F. M. Ashcroft (1999) Inwardly rectifying potassium channels *Curr Opin Cell Biol* **11** (4): 503-8.
- Ricardo Perez Riera, A., C. Ferreira, S. J. Dubner and E. Schapachnik (2004) Andersen syndrome: the newest variant of the hereditary-familial long QT syndrome *Ann Noninvasive Electrocardiol* **9** (2): 175-9.
- Roberts R: Mechanisms of disease: genetic mechanisms of atrial fibrillation. *Nature Clinical Practice Cardiovascular Medicine*, S. 276-282 (2006)
- Rudel, R., F. Lehmann-Horn, K. Ricker and G. Kuther (1984) Hypokalemic periodic paralysis: in vitro investigation of muscle fiber membrane parameters *Muscle Nerve* **7** (2): 110-20.
- Ruff, R. L. (1999) Insulin acts in hypokalemic periodic paralysis by reducing inward rectifier K<sup>+</sup> current *Neurology* **53** (7): 1556-63.
- Sanguinetti, M. C. and P. S. Spector (1997) Potassium channelopathies *Neuropharmacology* **36** (6): 755-62.
- Sansone, V., R. C. Griggs, G. Meola, L. J. Ptacek, R. Barohn, S. Iannaccone, W. Bryan, N. Baker, S. J. Janas, W. Scott, D. Ririe and R. Tawil (1997) Andersen's syndrome: a distinct periodic paralysis *Ann Neurol* **42** (3): 305-12.

- Schulze-Bahr, E. (2005) Short QT syndrome or Andersen syndrome: Yin and Yang of Kir2.1 channel dysfunction *Circ Res* **96** (7): 703-4.
- Seemann, G., F. B. Sachse, D. L. Weiss, L. J. Ptacek and M. Tristani-Firouzi (2007) Modeling of IK1 mutations in human left ventricular myocytes and tissue *Am J Physiol Heart Circ Physiol* **292** (1): H549-59.
- Shyng, S. L., C. A. Cukras, J. Harwood and C. G. Nichols (2000) Structural determinants of PIP(2) regulation of inward rectifier K(ATP) channels *J Gen Physiol* **116** (5): 599-608.
- Signorini, S., Y. J. Liao, S. A. Duncan, L. Y. Jan and M. Stoffel (1997) Normal cerebellar development but susceptibility to seizures in mice lacking G protein-coupled, inwardly rectifying K<sup>+</sup> channel GIRK2 *Proc Natl Acad Sci U S A* **94** (3): 923-7.
- Stanfield, P. R., N. W. Davies, P. A. Shelton, M. J. Sutcliffe, I. A. Khan, W. J. Brammar and E. C. Conley (1994) A single aspartate residue is involved in both intrinsic gating and blockage by Mg<sup>2+</sup> of the inward rectifier, IRK1 *J Physiol* **478** ( Pt 1): 1-6.
- Soom, M., R. Schonherr, Y. Kubo, C. Kirsch, R. Klinger and S. H. Heinemann (2001) Multiple PIP2 binding sites in Kir2.1 inwardly rectifying potassium channels *FEBS Lett* **490** (1-2): 49-53.
- Sung, H. K., T. Morisada, C. H. Cho, Y. Oike, J. Lee, E. K. Sung, J. H. Chung, T. Suda and G. Y. Koh (2006) Intestinal and peri-tumoral lymphatic endothelial cells are resistant to radiation-induced apoptosis *Biochem Biophys Res Commun* **345** (2): 545-51.
- Taglialatela, M., B. A. Wible, R. Caporaso and A. M. Brown (1994) Specification of pore properties by the carboxyl terminus of inwardly rectifying K<sup>+</sup> channels *Science* **264** (5160): 844-7.
- Tawil, R., L. J. Ptacek, S. G. Pavlakis, D. C. DeVivo, A. S. Penn, C. Ozdemir and R. C. Griggs (1994) Andersen's syndrome: potassium-sensitive periodic paralysis, ventricular ectopy, and dysmorphic features *Ann Neurol* **35** (3): 326-30.
- Tawil, R., L. J. Ptacek, S. G. Pavlakis, D. C. DeVivo, A. S. Penn, C. Ozdemir and R. C. Griggs (1994) Andersen's syndrome: potassium-sensitive periodic paralysis, ventricular ectopy, and dysmorphic features *Ann Neurol* **35** (3): 326-30.
- Tester, D. J., P. Arya, M. Will, C. M. Haglund, A. L. Farley, J. C. Makielski and M. J. Ackerman (2006) Genotypic heterogeneity and phenotypic mimicry among

- unrelated patients referred for catecholaminergic polymorphic ventricular tachycardia genetic testing *Heart Rhythm* **3** (7): 800-5.
- Tester, D. J., L. J. Kopplin, M. L. Will and M. J. Ackerman (2005) Spectrum and prevalence of cardiac ryanodine receptor (RyR2) mutations in a cohort of unrelated patients referred explicitly for long QT syndrome genetic testing *Heart Rhythm* **2** (10): 1099-105.
- Tinker, A., Y. N. Jan and L. Y. Jan (1996) Regions responsible for the assembly of inwardly rectifying potassium channels *Cell* **87** (5): 857-68.
- Tristani-Firouzi, M. (2004) Polymorphic ventricular tachycardia associated with mutations in KCNJ2 *Heart Rhythm* **1** (2): 242-3.
- Tristani-Firouzi, M. (2006) Andersen-Tawil syndrome: an ever-expanding phenotype? *Heart Rhythm* **3** (11): 1351-2.
- Tristani-Firouzi, M., J. L. Jensen, M. R. Donaldson, V. Sansone, G. Meola, A. Hahn, S. Bendahhou, H. Kwiecinski, A. Fidzianska, N. Plaster, Y. H. Fu, L. J. Ptacek and R. Tawil (2002) Functional and clinical characterization of KCNJ2 mutations associated with LQT7 (Andersen syndrome) *J Clin Invest* **110** (3): 381-8.
- Tristani-Firouzi, M. and M. C. Sanguinetti (2003) Structural determinants and biophysical properties of HERG and KCNQ1 channel gating *J Mol Cell Cardiol* **35** (1): 27-35.
- Vanderburgh, D. J., C. A. Ackerley, D. H. Lynn and R. C. Anderson (1987) The use of silver nitrate staining and backscattered electron imaging to visualize nematode sensory structures *Scanning Microsc* **1** (4): 1881-6.
- Wible, B. A., M. Tagliatela, E. Ficker and A. M. Brown (1994) Gating of inwardly rectifying K<sup>+</sup> channels localized to a single negatively charged residue *Nature* **371** (6494): 246-9.
- Wickman, K. and D. E. Clapham (1995) Ion channel regulation by G proteins *Physiol Rev* **75** (4): 865-85.
- Wickman, K., J. Nemeč, S. J. Gendler and D. E. Clapham (1998) Abnormal heart rate regulation in GIRK4 knockout mice *Neuron* **20** (1): 103-14.
- Xia, M., Q. Jin, S. Bendahhou, Y. He, M. M. Larroque, Y. Chen, Q. Zhou, Y. Yang, Y. Liu, B. Liu, Q. Zhu, Y. Zhou, J. Lin, B. Liang, L. Li, X. Dong, Z. Pan, R. Wang, H. Wan, W. Qiu, W. Xu, P. Eurlings, J. Barhanin and Y. Chen (2005) A Kir2.1 gain-of-function mutation underlies familial atrial fibrillation *Biochem Biophys Res Commun* **332** (4): 1012-9.

- Xu, F. (2003) Numerosity discrimination in infants: evidence for two systems of representations *Cognition* **89** (1): B15-25.
- Yang, J., Y. N. Jan and L. Y. Jan (1995) Determination of the subunit stoichiometry of an inwardly rectifying potassium channel *Neuron* **15** (6): 1441-7.
- Yoon, G., S. Oberoi, M. Tristani-Firouzi, S. P. Etheridge, L. Quitania, J. H. Kramer, B. L. Miller, Y. H. Fu and L. J. Ptacek (2006) Andersen-Tawil syndrome: prospective cohort analysis and expansion of the phenotype *Am J Med Genet A* **140** (4): 312-21.
- Zaritsky, J. J., D. M. Eckman, G. C. Wellman, M. T. Nelson and T. L. Schwarz (2000) Targeted disruption of Kir2.1 and Kir2.2 genes reveals the essential role of the inwardly rectifying K(+) current in K(+)-mediated vasodilation *Circ Res* **87** (2): 160-6.
- Zhang, L., D. W. Benson, M. Tristani-Firouzi, L. J. Ptacek, R. Tawil, P. J. Schwartz, A. L. George, M. Horie, G. Andelfinger, G. L. Snow, Y. H. Fu, M. J. Ackerman and G. M. Vincent (2005) Electrocardiographic features in Andersen-Tawil syndrome patients with KCNJ2 mutations: characteristic T-U-wave patterns predict the KCNJ2 genotype *Circulation* **111** (21): 2720-6.
- Zobel, C., H. C. Cho, T. T. Nguyen, R. Pekhletski, R. J. Diaz, G. J. Wilson and P. H. Backx (2003) Molecular dissection of the inward rectifier potassium current (IK1) in rabbit cardiomyocytes: evidence for heteromeric co-assembly of Kir2.1 and Kir2.2 *J Physiol* **550** (Pt 2): 365-72.

## ACKNOWLEDGMENTS

My special thanks to my supervisor Prof. Dr. Stephan Grissmer for giving me the opportunity to make my PhD in the Institute of Applied Physiology from Ulm University, for his willingness to involve me into such a large topic of projects. I thank him for his support in my research studies, his understanding and patience in discussions and answering to all possible questions and situations.

I would like to thank to the Leader of the Institute of Applied Physiology, Prof. Dr. Dr. h. c. Lehmann-Horn for his support in my research study. Special thanks for the kind gift of plasmids and the clinical features of the patients from ATS family obtained by PD Dr. Karin Jurkat-Rott.

I wish to thank to Dr. Heike Jäger and Dr. Oliver Wittekindt for their molecular biological and electrophysiological helpful discussions. Thanks to my former and present working team Dr. Eva Frei, Dr. Violeta Visan, Dr. Tobias Dreker, Dr. Isabell Spindler, Anselm Cornelius Hoppner, Sylvia Prütting, Zerrin Kuras, Jessica Blendin, Katharina Ruff for their scientific discussion, mental support and enjoyable social activities.

Special thanks to Michael Fauler and Boris Holzherr for their helpful and critical scientific discussion. My special thanks to Boris Holzherr because his precious advices, understanding and support helped me to gracefully overcome all difficulties.

To all members of the Institute of Applied Physiology, thank you for the friendly and nice working atmosphere.

My special thanks to my family and friends for their patience, moral support and understanding during my PhD.

## **PUBLISHED CONTRIBUTIONS**

Mouhat S, Teodorescu G, Daniel Homerick, Visan V, Wulff H, Wu Y, Grissmer S, Darbon H, De Waard M, and Sabatier JM (2006). Pharmacological profiling of *Orthochirus scrobiculosus* toxin 1 analogues with a trimmed N-terminal domain. *Mol Pharmacol.* **69(1)**:354-62

Rossokhin A, Teodorescu G, Grissmer S, and Zhorov BS (2006). Interaction of d-Tubocurarine with Potassium Channels: Molecular Modeling and Ligand Binding. *Mol Pharmacol.* **69(4)**:1356-65

**Teodorescu G**, Fauler M, Hang C, Topaloglu H, Lehmann-Horn F, Grissmer S, Jurkat-Rott K (2007). Clinical spectrum and function of Kir2.1 inward rectifier potassium channel (in preparation)